Cosmological Results and Implications in Effective DGP

by

Lik-Neng Nathan Chow

A thesis

presented to the University of Waterloo

in fulfilment of the

thesis requirement for the degree of

Master of Science

in

Physics

Waterloo, Ontario, Canada, 2008

Author's Declaration

I hereby declare that I am the sole author of this thesis. This is a true copy of the thesis, including any required final revisions, as accepted by my examiners.

I understand that my thesis may be made electronically available to the public.

Abstract

We study a simple extension of the decoupling limit of boundary effective actions for the Dvali-Gabadadze-Porrati model, by covariantizing the π lagrangian and coupling to gravity in the usual way. This extension agrees with DGP to leading order in Mpl^{-1}, and simplifies the cosmological analysis. It is also shown to softly break the shift symmetry, while still being consistent with solar system observations. The generally covariant equations of motion for π and the metric are derived, then the cosmology is developed under the Cosmological Principle. Three analytic solutions are found and their stability is studied. Interesting DGP phenomenology is reproduced, and we consider one of the stable solutions. The cosmological analogue of the Vainshtein effect is reproduced and the effective equation of state, w_π, is shown to be bounded by -1 from above. This solution is additionally shown to be an attractor solution in an expanding universe. We evolve π numerically and reproduce these properties, and show that the universe will go through a contraction phase, due to this π field. We then place a constraint on $r_c \geq 10^{29}$ cm, given recent WMAP5 data. This lower bound on r_c gives an upper bound on the anomalous perihelion precession of the moon $\sim 1 \times 10^{-13}$, 2 orders of magnitude below current experimental precision.

Acknowledgements

The author is grateful for Justin Khoury and his limitless guidance, patience, and understanding. The author is also overwhelmed by Nele Michiels and her unconditional support and compassion. Additional thanks is extended to Mark Wyman for his assistance with numerical integration techniques, and to Alberto Nicolis for his clarification on broken shift symmetries.

Dedication

This thesis is dedicated to the memory of Dyna Holtze, whose force of attraction will never be modified and mysterious source of energy never explained.

Contents

List of Figures

Chapter 1

Introduction

Perhaps the most important conceptual problem in cosmology today, is the observational inference of dark energy. It is thought to comprise over 70% of our universe's energy density, a value determined by the observed accelerated expansion of the universe [1]. Cosmic acceleration is now firmly established through observations of the Cosmic Microwave Background (CMB) anisotropy, Type Ia supernovae, and baryon acoustic oscillations, and requires explanation [2, 3, 4]. It is generally attributed to vacuum energy, with models that use a cosmological constant Λ, and cold dark matter (ΛCMD) [1, 5, 6, 7]. However, an alternative explanation is that Einstein's theory of gravity is breaking down on the largest observable scales. To reconcile the increased expansion rate at large range with theory, the former assumes an effective repulsive force between cosmological objects at large distances, while the latter postulates a weakening of the gravitational force at large distances.

It has proven, however, theoretically challenging to consistently alter Einstein gravity at large distances. One of the rare examples is the Dvali-Gabadadze-Porrati

(DGP) model [8]. In this scenario, our visible universe is confined to a brane in a 4+1-dimensional bulk. Although the bulk is flat and infinite in extent, 3+1-dimensional gravity is recovered, at least at sufficiently small distances, due to an intrinsic Einstein-Hilbert term on the brane. The full 5d action therefore takes the form

$$S_{\rm DGP} = \frac{M_5^3}{2}\int_{\mathcal{M}_5} d^5x\sqrt{-g_5}R_5 + \frac{M_4^2}{2}\int_{\mathcal{M}_4} d^4x\sqrt{-g_4}R_4 + M_4^2\int_{\mathcal{M}_4} d^4x\sqrt{-g_4}K\,, \quad (1.1)$$

where M_4 and M_5 respectively denote the 4d and 5d Planck scales, and K is the usual Gibbons-Hawking term [9] (see Fig. 1.1). In other words, the brane Ricci scalar represents an intrinsic graviton kinetic term that localizes the gravitational flux lines near the brane. The resulting gravitational force law scales as r^{-2} at short distances, but asymptotes to r^{-3}, corresponding to 4+1-dimensional behavior, at large distances. The cross-over scale is set by the ratio of the two Planck scales: $r_c = \frac{M_4^2}{M_5^3}$, as shown in Fig. 1.2. To satisfy solar system and cosmological constraints, r_c must be of order of the present Hubble radius: $\sim 10^{28}$ cm [10].

The DGP model is phenomenologically very rich. From the 4d effective theory on the brane, there is no massless graviton; instead the action is that of a resonance graviton — an infinite sum of massive states. The absence of a graviton zero-mode follows from the infinite extent of the bulk, which prevents the usual Kaluza-Klein mass gap between the graviton zero-mode and massive KK modes characteristic of compact extra dimensions.

At quadratic order, the action for the 4d graviton is of the Fiertz-Pauli (FP) form [11], except for the fact that the mass term is not constant but depends on 4d momentum: $m^2(p) = p^2 + \frac{p}{r_c}$. Theories of massive gravity have a long history. Fiertz

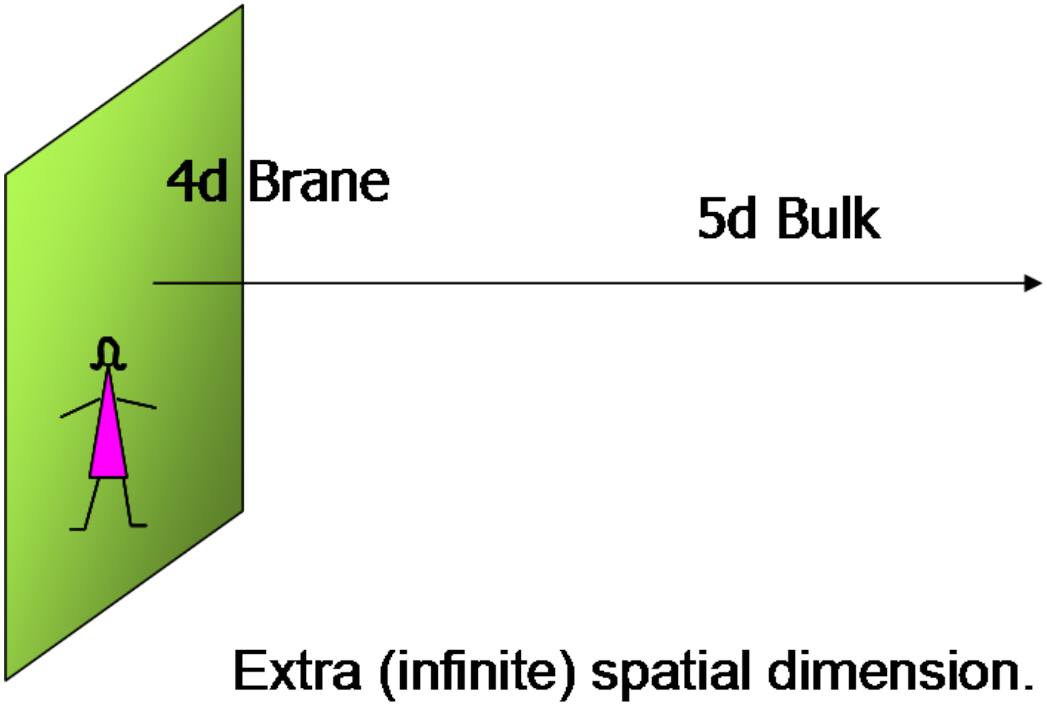

Figure 1.1: A visual depiction of the DGP framework.

and Pauli first showed that requiring Lorentz invariance and the absence of ghost-like instabilities uniquely fixes the tensor structure at quadratic order. Decades later, van Dam, Veltman and Zhakarov (vDVZ) pointed out that the resulting tensor structure of the one-particle exchange amplitude between conserved sources $T_{\mu\nu}$ and $T'_{\mu\nu}$ is that of a scalar-tensor (or Brans-Dicke [12]) theory [13]:

$$\mathcal{A} \sim \frac{1}{p^2 + m^2} \left(T^{\mu\nu} T'_{\mu\nu} - \frac{1}{3} T T' \right) , \tag{1.2}$$

By constrast, general relativity (GR) gives a coefficient of $\frac{1}{2}$ in front of the TT' term. The puzzling observation is that this $\frac{1}{3}$ coefficient persists even in the massless limit $m \to 0$ — surprisingly, the theory does not reduce to GR even in the limit of infinitesimal mass! Moreover, such a large departure from GR is already ruled out time-delay observations in the solar system, thus it would seem that a massive graviton of arbitrarily small mass is ruled out by solar system tests.

This vDVZ discontinuity arises because the longitudinal (or helicity-0) mode, usually denoted by π, does not decouple in the limit $m \to 0$. However, as pointed out by Vainshtein [14], π becomes non-linear in the vicinity of astrophysical sources. In other words, the linearized approximation assumed in Eq. (1.2), while applicable to the helicity-2 (or Einsteinian) part of the metric, in fact breaks down near the Sun. The scale at which perturbative theory breaks down in massive gravity is given by the Vainshtein radius: $r_{\rm V} = (r_{\rm Sch} m^{-4})^{1/5}$, where $r_{\rm Sch}$ is the Schwarzschild radius of the source. Vainshtein conjectured that due to these non-linear effects GR would be recovered for $r \ll r_{\rm V}$. Since $r_{\rm V} \to \infty$ as $m \to 0$, GR would recover everywhere in this limit. However it is clear that the recovery of GR is rather tricky, since it hinges on one of the degrees of freedom becoming strongly coupled everywhere.

The DGP model shares many of the key features of massive gravity. At the linearized level, the exchange amplitude between sources on the brane is of the form Eq. (1.2), except for the trivial substitution $m^2 \to r_c^{-1} p$. However, the longitudinal mode π is non-linear below a scale $r_\star$, which is the analogue of the Vainsthein radius:

$$r_\star = (r_{\rm Sch} r_c^2)^{1/3} \,. \tag{1.3}$$

And indeed, it has been shown that the Vainshtein effect applies in DGP: the standard Schwarzschild metric is recovered near sufficiently massive sources, plus correction suppressed by powers of $\frac{r}{r_\star}$ [15, 16, 17]. A conceptual analogue is to think of sound waves propagating through a dense 2d medium, surrounded by air. At short distances, the sound wave will be confined to the 2d 'brane' because of its large density. This is the scale that $r_\star$ defines, the so-called Einstein sphere, as GR is recovered exactly within. At large distances the sound waves will leak into the 3d bulk, the scale r_c defines, the distance at which gravity becomes 4+1 dimensional. Between $r_\star$ and r_c this is a complicated region where the theory is a scalar-tensor theory (see Fig. 1.2). In the sound analogy, if 2d beings existed on this 'brane' they would observe a 'modified sound law' after some scale, due to the 3d leaking. This is potentially our current position in our historical understanding of gravity.

Much work has been done to study the cosmology of the DGP model. Assuming a spatially-flat universe for simplicity, the Friedmann equation on the brane is given by [18]

$$H^2 = \frac{8\pi G}{3}\rho \pm \frac{H}{r_c} \,, \tag{1.4}$$

where ρ is the energy density of matter fields on the brane. Much attention has been paid to the "plus" (or self-accelerating) branch of this equation, because of its asymp-

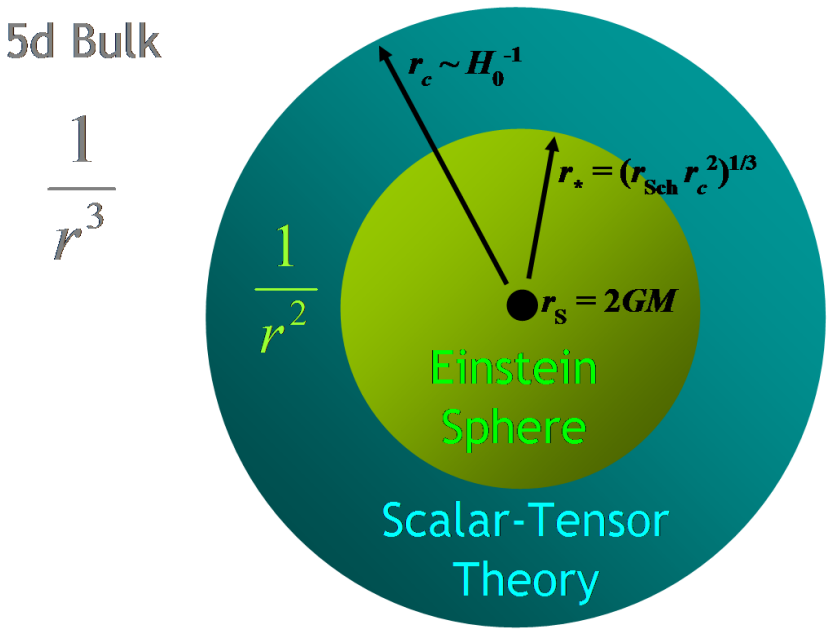

Figure 1.2: The regimes of interactions for a gravitational source in DGP.

totically de Sitter solution even in the absence of vacuum energy. However, various arguments have by now firmly established that this branch suffers from instabilities [19, 20, 21, 22, 23]. Here we instead focus on the "minus" or normal branch, which is stable. In this case, the $\frac{1}{Hr_c}$ correction slows down the expansion rate, and one must invoke a cosmological constant or some other form of dark energy to generate cosmic acceleration.

The cosmological viability of the DGP model has been the subject of a large body of literature, focusing almost exclusively on the self-accelerating (or plus) branch [24, 25, 26, 27, 28, 29]. Recently, [30] has shown that self-accelerating DGP cosmology is strongly disfavored compared to ΛCDM, due to modifications in the expansion and growth histories. Even allowing for spatial curvature to alleviate the tension with the expansion history, the modification to the growth of perturbations still generates too large an Integrated Sachs-Wolfe component for the low multipoles of the CMB angular power spectrum. Although this analysis focused on the plus branch, we expect the excess of power at large angular scales to also afflict the normal branch [31].

In general, the study of cosmology has been hampered by the sheer complexity of studying perturbations in a higher-dimensional space-time. In this thesis, we will use a specific limit in which the theory admits a local, four-dimensional description. This limit exploits the fact that near sources the non-linearities are dominated by those of π. Thus, by taking $M_4, M_5 \to \infty$ and $r_c \to \infty$, but keeping the strong coupling scale $\Lambda = (M_4 r_c^{-2})^{1/3}$ fixed, one decouples gravity but treats π non-linearly. In other words, this limit corresponds to taking $r_{\rm Sch} \to 0$, thus making helicity-2 modes weakly coupled everywhere, but keeping $r_\star$ fixed, thereby focusing on the π non-linearities. This so-called decoupling limit was first used in [32] and [33].

In [20], it was shown that the decoupling limit reproduces many of the key features of the full DGP model. In particular, it displays the Vainshtein effect through the non-linear interactions of π; it has both flat and self-accelerated solutions. More generally, solutions to the decoupled theory come in two branches, set by a choice of sign in the π equation of motion. (In the higher dimensional theory, this corresponds to a choice of sign of the extrinsic curvature of the brane.) One branch of solutions has stable perturbations, whereas the other branch is unstable. The asymptotically flat and self-accelerations solutions are a particular example of such pairs of solutions. Classically, the two branches are disconnected, unless the matter violates some energy condition [20]. It remains an open question whether quantum mechanical transitions can connect them [23, 24].

In this thesis, we study a simple extension of the decoupling theory, by covariantizing the π Lagrangian and coupling to gravity in the usual way. This offers the simplest non-linear and generally covariant extension, which agrees with DGP to leading order in $1/M_4$. Our approach has the advantage of being four-dimensional, which greatly simplifies the cosmological analysis.

Despite its remarkable simplicity, our 4d theory reproduces many of the key features of the full-fledged DGP model. Our Friedmann equation allows two branches of solutions, depending on the sign of the velocity of π. One branch corresponds to self-acceleration, the other is asymptotically flat. As in standard DGP, the self-accelerated and flat branches are unstable and stable, respectively. The π field contributes an effective energy density to the Friedmann equation on the stable (unstable) branch which has an effective equation of state $w < -1$ ($w > -1$), in agreement with [34].

Moreover, the π field displays a cosmological analogue of the Vainshtein effect.

In the presence of a background fluid, such as matter or radiation, the π dynamics are dominated by its non-linear interactions at early times ($Hr_c \gg 1$); the resulting effective energy density is then suppressed compared to the background fluid. In this regime where the π field is subdominant, we analytically derive a tracking solution in which $\dot{\pi}$ is constant. Furthermore, we show that it is an attractor, as small perturbations redshift away. We then check numerically the existence of this tracking solution and its attractor property. We numerically determine the effect on the total equation of state $w_{\rm tot}$, and show the universe will go through a contraction phase, due to this π field. We additionally show that for the majority of the evolution, w_π tracks $w_{\rm tot}$, as expected from the $\dot{\pi}$ is constant analysis. As a concluding calculation, we place a rough (yet stronger) constraint on $r_c \geq 10^{29}$ cm, using WMAP5 constraints on Ω_Λ and $w_{\rm DE}$, as well as our numerical model.

This thesis is organized in the following manner; In Chapter 2, we provide further background and motivation of DGP and its 4d effective models. In Chapter 3, we make generalizations to the 4d effective action in [20], in an effort to covariantize it. Requirements of stability place restrictions on how general an action we can have, and we pick a simple covariant action which satisfies these requirements. In Chapter 4, we develop its theoretical framework, then assume homogeneity and isotropy to calculate our modified equations of motion and Friedmann equations. In Chapter 5, we determine a handful of analytical solutions to these equations and discuss their stability and evolution, making contact with discussions in Chapter 2. Finally, in Chapter 6 we evolve these equations numerically in order to determine the cosmology for an arbitrary solution set. We show the validity of our analytic analysis in Chapter 5, and discuss the cosmological implications of this model.

Chapter 2

Background and Motivation

We start by describing the DGP model, and its main properties. Three scales of interest exist in this model; the scale at which the gravity looks 4d, the scale at which non-linear terms become important, and the scale that the theory becomes strongly coupled and loses predictivity. We present the unstable "self-accelerating" solution[1]. The discussion is then turned to the boundary effective action of Luty, Porrati, and Rattazzi [33], in which the 4+1 bulk has been integrated out, and its dynamics appear as a π field scalar degree of freedom, on the boundary. We make note of the useful decoupling limit [32, 33], then move to the Nicolis and Rattazzi (NR) truncated π action [20], which immediately reveals the LPR action's interesting structure. We show that the NR action is free of $n > 2$ higher order derivatives, and invariant under the shift symmetry. We end this chapter by discussing the observation viability of DGP (and its 4d effective models), in terms of solar system phenomenology.

[1]By "self-accelerated", we mean the de Sitter solution without vacuum energy or cosmological constant.

2.1 The Dvali-Gabadadze-Porrati Model

In the DGP model, our visible universe is confined to a brane in a 4+1-dimensional bulk. The bulk is flat and infinite in extent, and gravity is purely Einstein-Hilbert. There is a large Einstein-Hilbert term localized on the brane, which allows 3+1-dimensional gravity to be recovered at sufficiently small distances. The full 5d action is given by

$$S_{\rm DGP} = \frac{M_5^3}{2}\int_{\mathcal{M}_5} d^5x\sqrt{-g_5}R_5 + \frac{M_4^2}{2}\int_{\mathcal{M}_4} d^4x\sqrt{-g_4}R_4 + M_4^2\int_{\mathcal{M}_4} d^4x\sqrt{-g_4}K\,, \quad (2.1)$$

where M_4 and M_5 respectively denote the 4d and 5d Planck scales, and K is the Gibbons-Hawking term. The crossover scale between 3+1-dimensional gravity and 4+1-dimensional gravity is set by the ratio of these two Planck scales,

$$r_c = \frac{M_4^2}{M_5^3}. \quad (2.2)$$

At distances shorter than r_c (in the 3+1-dimensional regime), we have the usual gravitational force law r^{-2}. But at distances larger than r_c, gravity leaks into the 4+1 dimensional bulk, and we have the modified gravitational force law r^{-3}. A conceptual analogue is to think of sound waves propagating through a dense 2d medium, surrounded by air. At short distances, the sound wave will be confined to the 2d 'brane' because of its large density, but at large distances the sound waves will leak into the 3d bulk. If 2d beings existed on this 'brane' they would observe a 'modified sound law' after some scale, due to the 3d leaking[2]. This is precisely the scale that r_c defines, in DGP. To satisfy solar system and cosmological constraints, r_c must be of order of the present Hubble radius: $\sim 10^{28}$ cm [10] (which we will show in Section 2.3).

[2]Credit to G. R. Dvali for this thought experiment.

This, however, is not the complete story for distances $< r_c$. The DGP model reduces to a 4d scalar-tensor theory of gravity in this limit, where the scalar π, couples to the gravitational strength. This coupling survives even in the limit of $m \to 0$, which means that DGP does not limit to GR at distances smaller than r_c! This is precisely the vDVZ discontinuity which appears in theories of massive gravity [13]. One would expect then, that DGP would suffer the same fate as massive gravity theories, and predict unacceptable deviations from observational constraints placed on general relativity. Vainshtein [14], however, showed in massive gravity that, at distances close to an astrophysical source (such as the Sun), π becomes non-linear. The scale at which the non-linear terms become important is the Vainshtein radius:

$$r_{\rm V} = (r_{\rm Sch} m^{-4})^{\frac{1}{5}}, \tag{2.3}$$

where $r_{\rm Sch}$ is the Schwarzschild radius of the source. He claimed that the non-linear effects of π actually restore predictions to that of GR, and that GR would be fully recovered for $r \ll r_{\rm V}$. Since $r_{\rm V} \to \infty$ as $m \to 0$, GR is recovered everywhere in this limit. Such was the case in massive gravity, and it is indeed true that DGP suffers the same fate. An analogous Vainshtein radius exists for DGP, in which π becomes non-linear, and GR is recovered[3,4]! This scale is given by,

$$r_\star \sim \left(r_{\rm Sch} r_c^2\right)^{\frac{1}{3}}, \tag{2.4}$$

and is an important length scale in this theory, and its effective models, for the reasons above.

As shown in [33], there is a final additional length scale of importance, in DGP.

[3] With corrections suppressed by powers of $r/r_\star$. See [15, 16, 17].

[4] In Section 2.3, we will show this explicitly for the Sun.

It is the scale where the theory becomes strongly coupled and quantum mechanical effects come to dominate,

$$\Lambda \sim \frac{M_5^2}{M_4} = \left(\frac{M_4}{r_c^2}\right)^{\frac{1}{3}}. \tag{2.5}$$

Below this length, one cannot trust calculations done in the DGP framework without UV completion [38]. For r_c of order of the present Hubble radius, Λ^{-1} corresponds to $\sim 10^3$ km.

For late time cosmology, the DGP model has a "self-accelerating" branch, which can be seen by the modified Friedmann equation [18],

$$H^2 = -\frac{k}{a^2} + \left(\frac{\epsilon}{2r_c} + \sqrt{\frac{1}{4r_c^2} + \frac{8\pi G\rho}{3}}\right)^2, \tag{2.6}$$

where ρ is the energy density of matter fields on the brane. For $\epsilon = +1$ the r_c terms can act as a cosmological constant. This solution attracted a lot of attention because of this naturally occurring effective vacuum energy, without the need to put a cosmological constant in by hand. However, it has now been established that this branch suffers from instabilities [19, 20, 21, 22, 23][5]. Here we instead focus on the $\epsilon = -1$, or normal branch, which is stable. We will, however, reproduce the analogue to this "self-accelerated" solution in our 4d effective theory.

The study of the cosmology of this stable branch is notoriously difficulty. This is due to the complexity of studying perturbations in a higher-dimensional space-time. The natural step then, is to produce a 4d effective theory which reproduces the interesting phenomenology of DGP, while simplifying the calculations. This was first done by Luty, Porrati, and Rattazzi, whose model we will now describe.

[5]It has been conjectured the whole theory is not bounded from below, and thus unstable [23].

2.2 The Luty-Porrati-Rattazzi Effective Model

The first successful attempt at capturing the interesting phenomenology of the DGP model was the Luty-Porrati-Rattazzi (LPR) boundary effective action. This was done by integrating out the bulk degrees of freedom and encapsulating them into a single 4d scalar degree of freedom $\pi(x)$. π is often referred to as the "brane-bending" mode, and represents the 4+1-dimensional bulk dynamics of DGP on the boundary. The calculation is long and involved, but amounts to choosing convenient gauges and applying the Israel junction conditions between the bulk and the brane. The first step is to write the 4+1 part of the action in terms of ADM-like variables: the lapse $N = \left(g^{55}_{(5)}\right)^{-\frac{1}{2}}$, the shift $N_\mu = g_{(5)5\mu}$ and the 4d metric $g_{(4)\mu\nu} = g_{(5)\mu\nu}$;

$$S_{\mathrm{DGP}(5)} = \frac{M_5^3}{2}\int d^4x \int_0^\infty dy \sqrt{-g_{(4)}} N \left[R\left(g_{(4)}\right) - K^{\mu\nu}K_{\mu\nu} + K^2\right], \tag{2.7}$$

where

$$K_{\mu\nu} = \frac{1}{2N}\left(\dot{g}_{(4)\mu\nu} - \nabla_{(4)\mu}N_\nu - \nabla_{(4)\nu}N_\mu\right). \tag{2.8}$$

Choose the de Donder gauge for both metrics,

$$g_{(5)\mu\nu} = \eta_{(5)\mu\nu} + h_{(5)\mu\nu}, \tag{2.9}$$

$$g_{(4)\mu\nu} = \eta_{(4)\mu\nu} + h_{(4)\mu\nu}. \tag{2.10}$$

One is now in the position to integrate out the bulk fields, using the Israel junction conditions to match the bulk to the boundary[6], gives the induced boundary action. Adding this to the kinetic term on the boundary gives the quadratic boundary La-

[6]It is also convenient to add a gauge fixing term, and note the condition the residual gauge freedom has, but for brevity this has not been reproduced here. See [33, Section 3] for details.

grangian,

$$S_{\rm LPR} \simeq M_4^2 \int d^4x \left(\frac{1}{2} h'^{\mu\nu} \Box h'_{\mu\nu} - \frac{1}{4} h' \Box h' - m N^\mu \triangle N_\mu + 3m^2 \pi \Box \pi \right) - M_5^3 \int d^4x \, (\partial\pi)^2 \Box \pi, \tag{2.11}$$

where $\triangle = \sqrt{-\Box} = \sqrt{-\eta^{\mu\nu}\partial_\mu\partial_\nu}$, and $h'_{\mu\nu} = h_{(4)\mu\nu} - m\pi\eta_{(4)\mu\nu}$, and we have assumed that $p \gg m$.

To study the strong interactions regime, one can take the decoupling limit, M_4, $M_5 \to \infty$, while requiring Λ to be fixed, which sends $m \to 0$. This decoupling limit is analyzed in the detail by Nicolis and Rattazzi, in flat space [20]. These conditions reduce Eq. (2.11) to,

$$S_{\rm NR} = \int d^4x \left[-3(\partial\pi)^2 - \frac{1}{\Lambda^3} (\partial\pi)^2 \Box\pi + \frac{T\pi}{2M_4} \right]. \tag{2.12}$$

The first variation with respect to π shows that the resulting π equation of motion is given by,

$$3\Box\pi + \Lambda^{-3} \left[(\Box\pi)^2 - (\partial_\mu\partial_\nu\pi)^2 \right] = -\frac{T}{4M_4}, \tag{2.13}$$

which is remarkably free of $n > 2$ derivatives[7].

One can also show that this action is invariant under the shift symmetry,

$$\nabla_\mu\pi \to \nabla_\mu\pi + C_\mu, \tag{2.14}$$

which implies,

$$(\partial\pi)^2 \to (\partial\pi)^2 + 2C^\mu\nabla_\mu\pi + C^2, \tag{2.15}$$

$$\Box\pi \to \Box\pi. \tag{2.16}$$

[7]We will discuss this property more generally in Chapter 3.

Under this transformation, $\mathcal{L}_{\rm NR}$ from Eq. (2.12) becomes,

$$\begin{aligned}\mathcal{L}'_{\rm NR} &= -3(\partial\pi)^2 - \Lambda^{-3}(\partial\pi)^2\Box\pi + \frac{T\pi}{2M_4} \\ &\quad -6C^\mu\nabla_\nu\pi\Box\pi - 3C^2 - \Lambda^{-3}\left[2C^\mu\nabla_\nu\pi\Box\pi + C^2\Box\pi\right], \end{aligned} \tag{2.17}$$

and all the extra terms are either total derivatives which disappear upon integration, or constants which disappear upon variation. This is simply equivalent to saying that the π of motion in Eq. (2.13) is dependent only on second derivatives of π. But it is a useful exercise to show this explicitly at the level of the action, in anticipation of generalizing Eq. (2.12) in Section 3.1, and breaking this shift symmetry in Section 3.2.

Nicolis and Rattazzi have shown that this truncated action captures DGP for a wide range of cosmological regimes, however it is only valid in flat space and for non-relativistic matter sources [20]. In the next chapter we will try to extend this effective action to curved space and relativistic matter sources, by covariantizing it and softening the decoupling limit, but first we will remark on the phenomenological consistency of DGP and this truncated boundary effective action.

2.3 Solar System Consistency

The reason DGP is interesting is because it is observationally a viable alternative to GR. It is consistent with our strongest constraints: solar system phenomenology. Much work has been done to verify this consistency due to the Vainshtein effect [10, 15, 35, 36]. One can estimate the relative correction to the gravitational potential[8] by showing that the scale $r_\star$ at which the non-linear interactions of $\chi(r)$, the longitudinal graviton, become comparable to the linear interactions for

$$r_\star = \left(r_{\rm Sch} r_c^2\right)^{\frac{1}{3}} . \tag{2.18}$$

By requiring this to smoothly match the linear regime, and approximating the solution inside $r_\star$ as an analytic series in r_c^{-1}, one can determine the leading behaviour of $\chi(r)$ for distances $r \ll r_\star$,

$$\chi(r \ll r_\star) \sim \frac{r_{\rm Sch}}{r_\star}\left(\frac{r}{r_\star}\right)^{\frac{1}{2}} , \tag{2.19}$$

which has the following relative gravitational potential correction,

$$\delta \sim \frac{r}{r_c}\sqrt{\frac{r}{r_{\rm Sch}}}. \tag{2.20}$$

For the Earth, $r_{\rm Sch} = 0.886$ cm, the Earth-Moon distance is $r = 3.84 \times 10^{10}$ cm, and $r_c = 10^{28}$ cm, this gives an anomalous perihelion precession of the moon $\sim 1 \times 10^{-12}$, while current observational limits are of the order $\sim 1 \times 10^{-11}$. This effect, however, may be observable in the near future, as there is to be expected a ten-fold increase of precision in the next set of Lunar Laser Ranging experiments [10, 36].

A thematically similar, but different consistency check can be done with Eq. (2.12), by computing the $r_\star$ effect due to the Sun [20]. We consider a static point-like source

[8] As was done in [36].

of mass M, $T = -M\delta^3(\vec{x})$, and look for a general, static, spherically symmetric solution. Then Eq. (2.13) becomes,

$$\vec{\nabla} \cdot \left[6\vec{E} + \hat{r}\frac{4}{\Lambda}\frac{E^2}{r} \right] = \frac{M}{2M_4}\delta^3(\vec{x}), \tag{2.21}$$

where $\vec{E} \equiv \vec{\nabla}\pi \equiv \hat{r}E(r)$. Integrate over a sphere centered at the origin, and this yields the following solutions to the resulting quadratic equation,

$$E_{\pm}(r) = \frac{\Lambda^3}{4r}\left[\pm\sqrt{9r^4 + \frac{1}{2\pi}r_c^3 r} - 3r^2 \right]. \tag{2.22}$$

At distances close to the source, the two solutions reduce to,

$$E_{\pm}(r \ll r_\star) = \pm\frac{\Lambda^3}{4\sqrt{2\pi}}\frac{r_\star^{\frac{3}{2}}}{r^{\frac{1}{2}}}, \tag{2.23}$$

which relates to a correction of the Newton force,

$$\frac{F_\pi}{F_{\text{Newton}}} \sim \left(\frac{r}{r_\star}\right)^{\frac{3}{2}} \sim \left(\frac{r^3}{r_{\text{Sch}}^{\odot}}\right)^{\frac{1}{2}}\frac{1}{r_c}. \tag{2.24}$$

Given $r_{\text{Sch}}^{\odot} \sim 10^5$ cm and $r_c \sim 10^{28}$ cm, even a correction of order 10^{-2} to the Newton force due to this fifth π force will not be observed unless $r \sim 10^{19}$ cm, far outside the solar system.

Thus, our strongest constraints do not observationally rule out the DGP model. It is a viable infrared modification to gravity, making it an interesting theory to study cosmological results and implications in. The rest of this thesis will be focused on this endeavour. We will start in the next chapter, by softening the decoupling limit used by LPR, as well as, Nicolis and Rattazzi, to covariantize the boundary effective action.

Chapter 3

4d Effective Action

In this chapter we generalize the LPR effective theory by making it covariant, extending it to curved space and relativistic dynamics. We also take a weaker decoupling limit, only requiring M_4 to be finite, instead of $M_4 \to \infty$. We determine what constraints are placed on a general 4d effective action, in order to ensure there are no $n > 2$ higher order derivatives. We also show how the shift symmetry is broken by our generalization. We then choose a simple covariant form of the action in Jordan frame and show how it limits to the LPR action and relates to the discussion which preceded it.

3.1 Constraints on Generalization

In Section 2.2, we saw that the LPR boundary effective model had the property of being free of $n > 2$ order higher derivatives. This is an important property to have, in order to avoid ghosts appearing in the higher derivative contributions to the action. In this section we will try to determine what class of effective actions has this property. We will make the following generalizations to the LPR model[1],

$$S_{\rm GLPR} = M^4 \int d^4x\sqrt{-g}\left[A(X) + B(X)D\left(Y\right)\right], \tag{3.1}$$

where $X \equiv M^{-4}(\partial\pi)^2$ and $Y \equiv \Lambda^{-3}\Box\pi$. Note that from now, we will work only in 3+1 dimensions, so the subscript on M_4 has been removed for brevity. We can make contact with Eq. (2.12), by $A(X) = -3X$, $B(X) = -X$, and $D\left(Y\right) = Y$.

The first variation of Eq. (3.1) with respect to π yields the following equation of motion,

$$\left[\nabla^\mu\pi\nabla_\mu\frac{dA}{dX} + \frac{dA}{dX}\Box\pi + \nabla^\mu\pi D\left(Y\right)\nabla_\mu\frac{dB}{dX} + \frac{dB}{dX}\nabla^\mu\pi\nabla_\mu D\left(Y\right) + \frac{dB}{dX}D\left(Y\right)\Box\pi\right]$$
$$- \frac{M^4}{2\Lambda^3}\nabla_\mu\left[\frac{dD}{dY}\nabla^\mu B(X) + B(X)\nabla^\mu\frac{dD}{dY}\right] = 0. \tag{3.2}$$

And we can immediately require $\frac{dD}{dY}$ to be constant, otherwise we are getting $n > 2$ higher derivatives in π, which we have no possibility of cancelling[2]. So

$$\frac{dD}{dY} = \text{constant}, \tag{3.3}$$

which we will call C. Substitution of this into Eq. (3.2), leaves us with the following $n > 2$ derivative terms,

$$\frac{C}{\Lambda^3}\frac{dB}{dX}\nabla^\mu\pi\nabla_\mu\Box\pi \quad \text{and} \quad -\frac{C}{\Lambda^3}\frac{M^4}{2}\Box B(X).$$

[1]For simplicity, we have set the Lagrangian for the matter field to zero.

[2]In a recent paper, [37], it was shown that there is a special class of more general combinations of functions $D\left(Y\right)$ and $B(X)$ that, in fact, do cancel $n > 2$ higher derivatives.

And we can expand $\frac{M^4}{2}\Box B(X)$ and show that the combination of these two terms result in no $n > 2$ derivatives,

$$\begin{aligned}\frac{M^4}{2}\Box B(X) &= \frac{2}{M^4}\frac{d^2B}{dX^2}\nabla_\nu\pi\nabla^\mu\nabla^\nu\pi\nabla_\alpha\pi\nabla_\mu\nabla^\alpha\pi \\ &\quad + \frac{dB}{dX}\left[(\partial_\mu\partial_\nu\pi)^2 + \nabla^\mu\pi\Box\nabla_\mu\pi\right]. \end{aligned} \tag{3.4}$$

In flat space the $\nabla_\mu\Box\pi$ and $\Box\nabla_\mu\pi$ terms precisely cancel[3]. We are left with no $n > 2$ order higher derivatives, which means that there are no additional constraints on $B(X)$. Thus, $B(X)$ can be an arbitrary function of $M^{-4}(\partial\pi)^2$. We should pause here to stress how unique this $(\partial\pi)^2\Box\pi$ structure is. Our action contained a second-order (covariant) derivative of π and we took the variation with respect to π. Yet for any arbitrary $B(X)$, the resulting action has no $n > 2$ order higher derivatives. Also note that there is no way in which $A(X)$ can contribute to higher order derivatives, which is not as surprising[4]. $A(X)$ is then a general function as well. For simplicity, we absorb the constant C from Eq. (3.3) into $B(X)$ which gives us the following form of our generalized LPR model,

$$S_{\rm GLPR} = M^4\int d^4x\sqrt{-g}\left[A(X) + \Lambda^{-3}B(X)\Box\pi\right], \tag{3.5}$$

which has been shown to be free of $n > 2$ order higher derivatives.

The analogue to the solar system phenomenology of Section 2.3 is as follows[5]; again we consider a static point-like source of mass m, $T = -m\delta^3(\vec{x})$, and look for a general, static, spherically symmetric solution. Then Eq. (3.2) becomes,

$$\vec{\nabla}\cdot\left[-2\frac{dA}{dX}\vec{E} - \hat{r}\frac{4}{\Lambda^3}\frac{dB}{dX}\Lambda\frac{E^2}{r}\right] = \frac{m}{2M}\delta^3(\vec{x}), \tag{3.6}$$

[3]This result holds in curved space, but you will pick up a term proportional to $R^\alpha_\mu\nabla_\alpha\pi$.
[4]$A(X)$ only contains first-order derivatives in the action.
[5]We have reinserted the matter field Lagrangian, the same one as in Eq. (2.12).

where $\vec{E} \equiv \vec{\nabla}\pi \equiv \hat{r}E(r)$. Integrate over a sphere centered at the origin, and this yields the following solutions to the resulting quadratic equation,

$$E_{\pm}(r) = -\frac{\Lambda^3}{4r}\left(\frac{dB}{dX}\right)^{-1}\left[\pm\sqrt{\left(\frac{dA}{dX}\right)^2 r^4 - \frac{1}{2\Lambda^3\pi}\frac{dB}{dX}\left(\frac{m}{M}\right)r} - \frac{dA}{dX}r^2\right]. \tag{3.7}$$

Again, we consider distances close to the source and all the $\frac{dA}{dX}$ terms are negligible compared to the $\frac{dB}{dX}$ term (they will be suppressed by a factor $\frac{r}{r_\star}$). The two solutions then reduce to,

$$E_{\pm}(r \ll r_\star) = \mp\frac{\Lambda^{\frac{3}{2}}}{\sqrt{2\pi}}\left(\frac{dB}{dX}\right)^{-1}\left[-\frac{dB}{dX}\left(\frac{m}{M}\right)r^{-1}\right]^{\frac{1}{2}}, \tag{3.8}$$

and we require[6] $\frac{dB}{dX} < 0$. The effect of $A(X)$ (or more correctly $\frac{dA}{dX}$) on $E_\pm$ is suppressed by a factor $\frac{r}{r_\star}$, for small distances from the source. Hence, its effect negligible for distances within the solar system. It follows from this, that the solar system consistency derived in Section 2.3 is recovered exactly.

[6] At least for $r \ll r_\star$.

3.2 Broken Shift Symmetry

In Section 2.2 we showed that the LPR effective action was invariant under Eq. (2.14). This shift symmetry represents a Galilean symmetry which is the decoupling remnant of the full 5D Lorentz symmetry[7]. Since the Galilean invariance is only approximate, we do expect Eq. (2.14) to be softly broken in the full DGP. In this section, we will show how general $A(X)$ and $B(X)$ break Eq. (2.14). Under transformations Eq. (2.15) and Eq. (2.16), $\mathcal{L}_{\rm GLPR}$ from Eq. (3.5) becomes,

$$\begin{aligned}
\mathcal{L}'_{\rm GLPR} &= M^4 A\left(M^{-4}\left[(\partial\pi)^2 + 2C^\mu\nabla_\mu\pi + C^2\right]\right) \\
&\quad + M^4\Lambda^{-3}B\left(M^{-4}\left[(\partial\pi)^2 + 2C^\mu\nabla_\mu\pi + C^2\right]\right)\Box\pi \\
&\approx M^4\left[A(X) + \Lambda^{-3}B(X)\Box\pi\right] \\
&\quad + \frac{1}{M^4}\left(\frac{dA}{dX} + \Lambda^{-3}\frac{dB}{dX}\Box\pi\right)\left(2C^\mu\nabla_\mu\pi + C^2\right). \qquad (3.9)
\end{aligned}$$

For a shift symmetric action, the third term would have to disappear, requiring $\frac{dA}{dX} =$ const. and $\frac{dB}{dX} =$ const., so that it can be split up into total derivatives and constants. This is precisely the form that Eq. (2.17) took. However, for arbitrary functions $A(X)$ and $B(X)$, the third term can not, in general, be put into this form. Then the shift symmetry is must be broken. This breaking, however, will be soft if $M \gg \Lambda$. To reproduce LPR in the limit $M_{\rm pl} \to \infty$, it is natural to identify $M = M_{\rm pl}$, which ensures that the shift symmetry is very softly broken for our general model, as it is in DGP.

[7] See [38, Section 5].

3.3 Covariant 4d Effective DGP

We now choose a simple covariant form of this $(\partial\pi)^2\Box\pi$ structure in Jordan frame. We have the freedom to choose an action which is simple in Einstein or Jordan frame, but we decide on Jordan frame because π does not couple to $T^{(\mathrm{m})}$ in this frame[8]. Hence, this is the frame in which we will be looking for cosmological results. We will, however, develop the resulting theoretical model of this action, in both frames. As a simple choice for a covariant completion of LPR, we choose the following action in Jordan frame,

$$S_{\mathcal{J}} = \int d^4x\sqrt{-g}\left[\frac{{M_{\rm pl}}^2}{2}R\Omega^{-2} - \Lambda^{-3}(\partial\pi)^2\Box\pi\right], \tag{3.10}$$

where $\frac{\Lambda}{\Lambda_{\rm LPR}} = \text{const}$. For the limit $M_{\rm pl} \to \infty$ and $\frac{\Lambda}{\Lambda_{\rm LPR}} = 1$, Eq. (3.10) reproduces LPR. To show this explicitly and make contact with the discussion in the preceding sections, we transform Eq. (3.10) into Einstein frame by the conformal transformation,

$$g_{\mu\nu} \;=\; \Omega^{-2}\tilde{g}_{\mu\nu}, \tag{3.11}$$

and note that,

$$\Box\pi = \Omega^2\left(\tilde{\Box}\pi - 2\tilde{\nabla}_\alpha\pi\tilde{\nabla}^\alpha\ln\Omega\right). \tag{3.12}$$

In anticipation of a kinetic term proportional to $(\partial\pi)^2$ and the conformal transformation of R we demand that $3{M_{\rm pl}}^2\Omega^{-5}\Box\Omega = 3\beta^2\Omega^{-2}\left(\tilde{\partial}\pi\right)^2$. This specifies our conformal factor as,

$$\Omega = e^{\beta{M_{\rm pl}}^{-1}\pi}, \tag{3.13}$$

where we have used Eq. (3.12) for $\Box\Omega$. Using Eq. (3.13) in Eq. (3.12) we will pick up an additional $(\partial\pi)^4$ term in this transformation. Our corresponding Einstein action

[8]This will be shown explicitly in Section 4.1.

then takes the following form

$$S_{\mathcal{E}} = \int d^4x\sqrt{-g}\left\{\frac{{M_{\rm pl}}^2}{2}R - 3\beta^2(\partial\pi)^2 - \Lambda^{-3}(\partial\pi)^2\left[\Box\pi + 2\beta {M_{\rm pl}}^{-1}(\partial\pi)^2\right]\right\}. \quad (3.14)$$

The sign in front of $(\partial\pi)^2$ is negative-definite, while the sign on $(\partial\pi)^2\Box\pi$ was chosen to be negative in accordance with Eq. (3.8). The DGP result explicitly specifies $\beta = +1$, which we will not enforce. This form of the action in Einstein frame corresponds to following functions in Eq. (3.5)[9],

$$A(X) = -3\beta^2(\partial\pi)^2 - 2\beta {M_{\rm pl}}^{-1}\Lambda^{-3}(\partial\pi)^4, \quad (3.15)$$

$$B(X) = -(\partial\pi)^2. \quad (3.16)$$

To take the LPR decoupling limit, $M_{\rm pl} \to \infty$, choose $\beta = +1$ and $\Lambda = \Lambda_{\rm LPR}$, and their model is recovered exactly.

We are now in the position to develop the theoretical and cosmological frameworks for our model using Eq. (3.10) and Eq. (3.14) as our actions in their respective frames.

[9]Further work with $A(X)$ and $B(X)$ as arbitrary functions can be found in the Appendix A.

Chapter 4

Field Equations and Cosmology

In Section 3.3, we chose particular forms of the 4d effective action in both Jordan and Einstein frame. In this chapter, we will derive the generally covariant equations of motion for π and the gravitational field for both actions, since it will be useful to go back and forth between these two frames. The Einstein frame is convenient because the gravitational sector is standard, with the Planck mass being constant. However, the matter stress tensor couples to π and is therefore not conserved. Conversely, the matter fields obey standard conservation equations in Jordan frame, but one must accept a space-time varying Planck scale. In each frame, we then specialize the equations of motion to the cosmological context, making the usual assumptions of homogeneity and isotropy. These will then be studied analytically and numerically in Chapters 5 and 6, respectively. There will be more emphasis put on Jordan frame, motivated by the discussion in Section 3.3. As such, we will additionally derive an alternate form for the π equation of motion and determine an effective w_π in the cosmological context, for Jordan frame.

4.1 Jordan Frame

We begin with the derivation of the covariant equation of motion of π in Jordan frame. In this frame the π field does not couple to the matter stress tensor, but instead it couples to the Ricci scalar. It has the advantage of the conservation equations of the matter fields being unaffected, but the Planck scale varies depending on Ω^{-2}. It is this advantage which we alluded to in Section 3.3, and will now explicitly show. We take the first variation with respect to π of the Jordan frame action given in Eq. (3.10),

$$\delta_\pi \mathcal{L}_\mathcal{J} \;=\; -\beta M_{\rm pl} R\Omega^{-2}\delta\pi + 2\Lambda^{-3}\nabla_\mu\left[\nabla^\mu\pi\Box\pi\right]\delta\pi - \Lambda^{-3}(\partial\pi)^2\Box\delta\pi. \tag{4.1}$$

Integration by parts and noting that $\nabla_\mu\Box\pi - \Box\nabla_\mu\pi = -R^\alpha_\mu\nabla_\alpha\pi$ give,

$$\beta M_{\rm pl} R\Omega^{-2} = 2\Lambda^{-3}\left[(\Box\pi)^2 - (\nabla_\mu\nabla_\nu\pi)^2 - \nabla^\mu\pi R^\beta_\mu\nabla_\beta\pi\right], \tag{4.2}$$

as our π equation of motion. And as discussed, the π field only couples to the Ricci scalar while $T^{(\rm m)}$ is left untouched.

To derive Einstein's equations, we start in the usual way by the first variation of Eq. (3.10) with respect to the metric,

$$\begin{aligned}\delta_g \mathcal{L}_\mathcal{J} \;=\; & \sqrt{-g}\left\{\frac{{M_{\rm pl}}^2}{2}\delta\left(R\Omega^{-2}\right) - \Lambda^{-3}\delta\left[(\partial\pi)^2\Box\pi\right]\right\} \\ & +\delta\left(\sqrt{-g}\right)\left[\frac{{M_{\rm pl}}^2}{2}R\Omega^{-2} - \Lambda^{-3}(\partial\pi)^2\Box\pi\right],\end{aligned} \tag{4.3}$$

with $\delta\left(R\Omega^{-2}\right) = \delta\left(R_{\mu\nu}\right)g^{\mu\nu}\Omega^{-2} + R_{\mu\nu}\delta g^{\mu\nu}\Omega^{-2}$, and noting that $\delta\left(\Omega^{-2}\right) = 0$. Two subtleties arise in this modified derivation;

First, $\sqrt{-g}\,\delta\left(R_{\mu\nu}\right)g^{\mu\nu}\Omega^{-2}$ is no longer a total derivative, as is the case in the Einstein frame derivation [39, Appendix E]. Accordingly, one must vary the Christoffels

in the full definition of $R_{\mu\nu}$ and then use integration by parts to find,

$$\delta\left(R_{\mu\nu}\right)g^{\mu\nu}\Omega^{-2} = \left(g_{\mu\nu}\Box\Omega^{-2} - \nabla_\mu\nabla_\nu\Omega^{-2}\right)\delta g^{\mu\nu}. \tag{4.4}$$

Second, a subtlety arises when calculating $(\partial\pi)^2\delta\Box\pi$, as another Christoffel appears and must too be varied,

$$(\partial\pi)^2\delta\Box\pi = \left[\nabla_\alpha\pi\left(g_{\mu\nu}\nabla^\beta\nabla^\alpha\pi\nabla_\beta\pi - 2\nabla_\mu\nabla^\alpha\pi\nabla_\nu\pi\right) + \frac{1}{2}g_{\mu\nu}(\partial\pi)^2\Box\pi\right]\delta g^{\mu\nu}. \tag{4.5}$$

Subsitution of Eq. (4.4) and Eq. (4.5) into Eq. (4.3) give

$$\begin{aligned}\Omega^{-2}G_{\mu\nu} &= {M_{\rm pl}}^{-2}T_{\mu\nu} + \nabla_\mu\nabla_\nu\Omega^{-2} - g_{\mu\nu}\Box\Omega^{-2} \\ &\quad + {M_{\rm pl}}^{-2}\Lambda^{-3}\left[2\nabla_\mu\pi\nabla_\nu\pi\Box\pi + g_{\mu\nu}\nabla_\alpha\pi\partial^\alpha(\partial\pi)^2 - 2\nabla_{(\mu}\pi\nabla_{\nu)}(\partial\pi)^2\right],\end{aligned} \tag{4.6}$$

as our Jordan frame field equations. If we neglect the second line, this corresponds to a Brans-Dicke theory with Ω^{-2} playing the role of ϕ and the Brans-Dicke parameter $\omega_{\rm BD} = 0$. Hence, our effective theory limits to a Brans-Dicke theory, for $\Lambda \to \infty$.

We can also derive an alternative form for the π equation of motion, by substituting for the Ricci scalar via,

$$\Omega^{-2}G^\mu_\mu = -R\Omega^{-2}. \tag{4.7}$$

Taking Eq. (4.7) in terms of Eq. (4.2), we substitute G^μ_μ into the trace of Eq. (4.6). This gives,

$$\begin{aligned}T^\mu_\mu &= 2\Lambda^{-3}\beta M_{\rm pl}\left[(\nabla_\mu\nabla_\nu\pi)^2 - (\Box\pi)^2 + \nabla^\mu\pi R^\beta_\mu\nabla_\beta\pi\right] \\ &\quad + 6\beta\Omega^{-2}\left[2\beta(\partial\pi)^2 - M_{\rm pl}\Box\pi\right] - 2\Lambda^{-3}\left[(\partial\pi)^2\Box\pi + \nabla_\mu\pi\partial^\mu(\partial\pi)^2\right].\end{aligned} \tag{4.8}$$

Which relates π to the trace of the stress energy tensor.

We now specialize this analysis to the cosmological context, by assuming homogeneity and isotropy, which demands π to only be a function of time. First we derive

the cosmological π equation of motion. Under these assumptions, Eq. (4.2) reduces to,

$$\frac{d}{dt}\left(H\dot{\pi}^2\right) + 3H\left(H\dot{\pi}^2\right) = \frac{1}{6}\beta M_{\rm pl}\Lambda^3 R\Omega^{-2}. \tag{4.9}$$

Or equivalently,

$$\frac{d}{dt}\Pi_{\mathcal{J}} + 3H\Pi_{\mathcal{J}} = R\Omega^{-2}, \tag{4.10}$$

where $\Pi_{\mathcal{J}} \equiv 6\beta^{-1}{M_{\rm pl}}^{-1}\Lambda^{-3}H\dot{\pi}^2$. This is precisely equivalent to the equation of a scalar field with canonical kinetic term, which couples to R, if we make the identification $\dot{\phi} \leftrightarrow \Pi_{\mathcal{J}}$.

We now turn our attention to the Friedmann equations, which are given by T_{00} and T_{ii}. We will see that the π field modifies the standard Friedmann equations by adding an effective energy density and pressure. For these derivations we will assume, as usual, that the matter is described by a perfect fluid:

$$T_{\mu\nu} = (\rho + P)u_\mu u_\nu + P g_{\mu\nu}, \tag{4.11}$$

where ρ and P denote the energy density and pressure of the fluid. Using (4.11) and the above assumptions of homogeneity and isotropy, we get the following modified Friedmann equations,

$$3{M_{\rm pl}}^2H^2 = \Omega^2\sum_i^n \rho_i + 6H\dot{\pi}\left(\beta M_{\rm pl} - \Omega^2\Lambda^{-3}\dot{\pi}^2\right), \tag{4.12}$$

and

$$\begin{aligned} {M_{\rm pl}}^2\left(2\frac{\ddot{a}}{a} + H^2\right) &= -\Omega^2\sum_i^n P_i + 2\beta\left[M_{\rm pl}\left(\ddot{\pi} + 3H\dot{\pi}\right) - 2\beta\dot{\pi}^2\right] \\ &\quad -2\Omega^2\Lambda^{-3}\dot{\pi}^2\ddot{\pi}. \end{aligned} \tag{4.13}$$

We can further combine these two equations to get the modified acceleration equation,

$$\begin{aligned}\frac{\ddot{a}}{a} &= -\frac{\Omega^2 {M_{\rm pl}}^{-2}}{6}\left\{\sum_i^n \rho_i + 3\sum_i^n P_i \right. \\ &\left. +3\left[\dot{\pi}^2\left(3\Lambda^{-3}\ddot{\pi}+4\beta^2\Omega^{-2}\right)-\left(\Lambda^{-3}\dot{\pi}^2+2\beta M_{\rm pl}\Omega^{-2}\right)\left(\ddot{\pi}+2H\dot{\pi}\right)\right]\right\}. \quad (4.14)\end{aligned}$$

From Eq. (4.12) and Eq. (4.13) we can also determine what the effective w for this π field is, by identifying ρ_π and P_π,

$$\rho_\pi = 6H\dot{\pi}\left(\beta M_{\rm pl}\Omega^{-2}-\Lambda^{-3}\dot{\pi}^2\right), \quad (4.15)$$

$$P_\pi = 2\Lambda^{-3}\dot{\pi}^2\ddot{\pi}-2\beta\Omega^{-2}\left[M_{\rm pl}\left(\ddot{\pi}+3H\dot{\pi}\right)-2\beta\dot{\pi}^2\right]. \quad (4.16)$$

From this we can infer an effective equation of state w_π for π, defined as usual as the ration of the pressure to the energy density:

$$w_\pi = -1+\frac{\Lambda^{-3}\dot{\pi}^2\left(\ddot{\pi}-3H\dot{\pi}\right)+\beta\Omega^{-2}\left(2\beta\dot{\pi}^2-M_{\rm pl}\ddot{\pi}\right)}{3H\dot{\pi}\left(\beta M_{\rm pl}\Omega^{-2}-\Lambda^{-3}\dot{\pi}^2\right)}, \quad (4.17)$$

is our effective w for the π field.

4.2 Einstein Frame

We now follow the same procedure in Einstein frame. In this frame, the gravitational sector of the action is as in Einstein gravity, in particular the Planck mass is constant, but the π field couples to the trace of the matter stress tensor. Start again with the π equation of motion by taking the first variation of Eq. (3.14) with respect to π,

$$\begin{aligned}\delta_\pi \mathcal{L}_\mathcal{E} &= -6\beta^2 \nabla_\mu \pi \nabla^\mu \delta\pi - 2\Lambda^{-3} \nabla_\mu \pi \nabla^\mu \delta\pi \Box\pi - \Lambda^{-3} (\partial\pi)^2 \Box\delta\pi \\ &\quad -2\beta {M_{\rm pl}}^{-1} \Lambda^{-3} \left(4 \nabla_\mu \pi \nabla_\nu \pi \nabla^\nu \pi \nabla^\mu \delta\pi\right). \end{aligned} \tag{4.18}$$

Integration by parts and noting that $\nabla_\mu \Box\pi - \Box \nabla_\mu \pi = -R^\alpha_\mu \nabla_\alpha \pi$ give,

$$\begin{aligned} &16\beta {M_{\rm pl}}^{-1} \Lambda^{-3} \nabla_\nu \pi \nabla_\mu \nabla^\nu \pi \nabla^\mu \pi + 2\Box\pi \left[3\beta^2 + 4\beta {M_{\rm pl}}^{-1} \Lambda^{-3} (\partial\pi)^2\right] \\ &\qquad +2\Lambda^{-3} \left[(\Box\pi)^2 - (\nabla_\mu \nabla_\nu \pi)^2 - \nabla^\mu \pi R^\beta_\mu \nabla_\beta \pi\right] = T^{(\rm m)}_\mathcal{E}. \end{aligned} \tag{4.19}$$

We see that π couples to the trace of the stress tensor, thus it mediates a fifth force between matter particles. In particular, in the absence of the non-linear terms, this fifth force would have a strength of order β^2 times that of gravity. As we have seen in Section 2.3 however, the non-linear terms play a crucial role in rendering the theory phenomenologically viable by suppressing the effects of π near astrophysical sources.

The field equations, are derived using Eq. (3.14) again, but now varying with respect to the metric,

$$\begin{aligned}\delta_g \mathcal{L}_\mathcal{E} &= \sqrt{-g} \left[\frac{{M_{\rm pl}}^2}{2} \delta R - 3\beta^2 \delta(\partial\pi)^2 - \Lambda^{-3} \delta(\partial\pi)^2 \Box\pi \right. \\ &\quad \left. -\Lambda^{-3} (\partial\pi)^2 \delta\Box\pi - 2\beta {M_{\rm pl}}^{-1} \Lambda^{-3} \delta \left(\partial\pi\right)^4\right], \end{aligned} \tag{4.20}$$

with $\delta R = \delta g^{\mu\nu} R_{\mu\nu} + g^{\mu\nu} \delta R_{\mu\nu}$. We note that $\sqrt{-g} \left(\delta R_{\mu\nu}\right) g^{\mu\nu}$ is a total derivative [39, Appendix E]. As in the Jordan frame derivation, $(\partial\pi)^2 \delta\Box\pi$ must be calculated

carefully.[1] Substituting Eq. (4.5) into Eq. (4.20) we get,

$$\begin{aligned} G_{\mu\nu} &= M_{\rm pl}{}^{-2}T_{\mu\nu} + 2M_{\rm pl}{}^{-2}\left[3\beta^2 - 4\beta M_{\rm pl}{}^{-1}\Lambda^{-3}(\partial\pi)^2\right]\nabla_\mu\pi\nabla_\nu\pi \\ &\quad -M_{\rm pl}{}^{-2}g_{\mu\nu}\left[3\beta^2(\partial\pi)^2 + 2\beta M_{\rm pl}{}^{-1}(\partial\pi)^4\right] \\ &\quad +M_{\rm pl}{}^{-2}\Lambda^{-3}\left[2\nabla_\mu\nabla_\nu\Box\pi + g_{\mu\nu}\nabla_\alpha\pi\partial^\alpha(\partial\pi)^2 - 2\nabla_{(\mu}\pi\nabla_{\nu)}(\partial\pi)^2\right], \end{aligned} \tag{4.21}$$

as our field equations.

We put these in the cosmological context and again start with the π equation of motion. Eq. (4.19) reduces to,

$$T_{\mathcal{E}}^{(\rm m)} = \frac{d}{dt}\Pi_{\mathcal{E}} + 3H\Pi_{\mathcal{E}}, \tag{4.22}$$

where $\Pi_{\mathcal{E}} \equiv 8\beta M_{\rm pl}{}^{-1}\Lambda^{-3}\dot\pi^3 + 6\Lambda^{-3}H\dot\pi^2 - 6\beta^2\dot\pi$. And this has the form of the equation of a scalar field with canonical kinetic term, which couples to $T_{\mathcal{E}}^{(\rm m)}$, if we make the identification $\dot\phi \leftrightarrow \Pi_{\mathcal{E}}$. Structurally the Einstein frame and Jordan frame π equation of motion are very similar, with the Ricci scalar playing the role of $T_{\mathcal{E}}^{(\rm m)}$.

We now turn our attention to the Friedmann equations, again given by T_{00} and T_{ii}. We will again assume Eq. (4.11) as in Jordan frame, to determine the corrections due to the π field.

$$3M_{\rm pl}{}^2H^2 = \sum_i^n \rho_i + 3\beta^2\dot\pi^2 - 6\Lambda^{-3}\dot\pi^3\left(H + \beta M_{\rm pl}{}^{-1}\dot\pi\right), \tag{4.23}$$

$$M_{\rm pl}{}^2\left(2\frac{\ddot a}{a} + H^2\right) = -\sum_i^n P_i - 3\beta^2\dot\pi^2 + 2\Lambda^{-3}\dot\pi^2\left(\beta M_{\rm pl}{}^{-1}\dot\pi^2 - \ddot\pi\right), \tag{4.24}$$

are our modified Friedmann equations in Einstein frame. We can combine these two equations in the usual way to get the modified acceleration equation,

$$\begin{aligned} \frac{\ddot a}{a} &= -\frac{M_{\rm pl}{}^{-2}}{6}\left\{\sum_i^n \rho_i + 3\sum_i^n P_i \right. \\ &\quad \left. +6\dot\pi^2\left[2\beta^2 + \Lambda^{-3}\left(\ddot\pi - 2\beta M_{\rm pl}{}^{-1}\dot\pi^2 - H\dot\pi\right)\right]\right\}. \end{aligned} \tag{4.25}$$

[1] See Eq. (4.5).

And these are our cosmological equations in Einstein frame.

We now attempt to find analytic solutions to the cosmological equations in Jordan frame, where we have purposefully choose an uncomplicated action.

Chapter 5

Analytical Results

Despite its remarkable simplicity, we will see in this chapter that our 4d scalar theory reproduces many of the key features of the full DGP model. In particular, we will derive both static and self-accelerated solutions. This shows that the self-accelerated solution of DGP is not unique to five-dimensional theories. More generally, our cosmological solutions come in two branches, which depend on the choice of sign for $\dot{\pi}$. As in DGP, the asymptotically trivial branch is stable, whereas solutions continuously connected to the self-accelerated cosmology have ghost-like instabilities. This also agrees with the conclusions reached by LPR in the decoupling limit.

5.1 Static and Self-Accelerating Solutions

In this section, we show that the vacuum solutions[1] allow two branches of solutions: a flat solution and a self-accelerated solution. For simplicity, we assume that $|\pi| \ll M_{\rm pl}$. We will check numerically in Chapter 6, that this is a consistent approximation, for a wide range of times. In this limit, $e^{-2\beta {M_{\rm pl}}^{-1}\pi} \to 1$, i.e. $\Omega^{-2} \approx 1$. For very late time cosmology this limit will break down, since π is growing and will eventually be of order $\sim M_{\rm pl}$. To seek a self-accelerated solution, we take as the ansatz that $H = H_0$ is a constant. Moreover, we will see that we can also take $\dot{\pi}$ to be constant,

$$3H_0^2\dot{\pi}^2 = \frac{1}{6}\beta M_{\rm pl}\Lambda^3 R. \tag{5.1}$$

One solution is clearly $H_0 = 0$. Substituting this solution into Eq. (4.13), gives $\dot{\pi} = 0$ as well. This is the flat, trivial branch that is seen in DGP. If, however, if we assume H is not zero, and use the fact that $R = 6H_0^2$ for constant H, we get;

$$\dot{\pi}^2 = \frac{1}{3}\beta M_{\rm pl}\Lambda^3, \tag{5.2}$$

$$\dot{\pi} = \alpha\left(\frac{\beta M_{\rm pl}\Lambda^3}{3}\right)^{\frac{1}{2}}, \tag{5.3}$$

with $\alpha = \pm 1$.

We can use Eq. (5.2) in Eq. (4.12), with $\sum_i^n \rho_i = 0$ to get,

$$H_0^2 = \frac{4}{3}\beta {M_{\rm pl}}^{-1} H_0\dot{\pi}, \tag{5.4}$$

and clearly the left hand side must be positive. If $\beta, H_0 > 0$, then α from Eq. (5.3) is forced to be $+1$. Hence, $\dot{\pi}$ must be positive. We can divide by H_0 on both sides and Eq. (5.4) reduces to

$$H_0 = \frac{4}{3}\beta {M_{\rm pl}}^{-1}\dot{\pi}, \tag{5.5}$$

[1] i.e. devoid of matter or radiation.

as the Friedmann equation in this limit. And we have found a self-accelerating solution in our 4d effective theory. This is exactly as in DGP. Thus the existence of a self-accelerated solution is not unique to higher dimensional gravity, but, as we have shown here, can be obtained in a scalar field theory with non-linear derivative interactions. Although not further developed in this thesis, one can imagine such a cleverly chosen 4d action could provide an alternative explanation of the vacuum energy problem, by having a stable self-accelerating solution.

5.2 Constant $\dot{\pi}$ Tracking Solution

We now move on to the more realistic case of the evolution of π in the presence of matter and/or radiation. We will assume the same simplifying Ω^{-2} approximation as with the static and self-accelerating solutions, and seek solutions where π is a subdominant component. We will see that the backreaction of π can be consistently neglected at early times, when $Hr_c \gg 1$. This makes sense since π is strongly coupled, and much like in the solar system phenomenology of Section 2.3, and its dynamics will be suppressed in this regime. For a background dominated by a fluid with constant equation of state w,

$$a = a_0 t^{\frac{2}{3(1+w)}}, \tag{5.6}$$

$$\dot{a} = a_0 \left[\frac{2}{3\left(1+w\right)}\right] t^{\frac{2}{3(1+w)}-1}, \tag{5.7}$$

$$R = 6\left(\frac{\ddot{a}}{a} + \frac{\dot{a}^2}{a^2}\right) = \frac{4\left(1-3w\right)}{3t^2\left(1+w\right)^2}. \tag{5.8}$$

Substitution of Eq. (5.6), Eq. (5.7), and Eq. (5.8) into Eq. (4.9) gives,

$$\dot{\pi}^2 + \frac{1+w}{1-w} t \frac{d}{dt}\dot{\pi}^2 = \frac{1}{3}\beta M_{\rm pl}\Lambda^3 \frac{1-3w}{1-w}, \tag{5.9}$$

and if we assume that $\dot{\pi}$ is constant in time the second term disappears. We can then analytically solve for $\dot{\pi}$,

$$\dot{\pi} = \alpha\left(\frac{\beta M_{\rm pl}\Lambda^3}{3}\frac{1-3w}{1-w}\right)^{\frac{1}{2}}. \tag{5.10}$$

For $\beta > 0$, this is only valid for $w \leq \frac{1}{3}$ (and $w > 1$). For $\beta < 0$, this is valid for $\frac{1}{3} \leq w < 1$. If w makes a transition so that these conditions are no longer satisfied, π will depart from the above solution, as our assumptions have broken down. Its evolution must then be solved numerically, as we will do in Chapter 6.

Let us now check to see whether our constant $\dot{\pi}$ solution is an attractor. We will analyze π fluctuations for this solution by perturbing Eq. (4.9) about $\dot{\pi} = \dot{\bar{\pi}} + \delta\dot{\pi}$,

$$2\dot{\bar{\pi}}\left[\frac{d}{dt}\left(H\delta\dot{\pi}\right) + 3H\left(H\delta\dot{\pi}\right)\right] = 0, \tag{5.11}$$

where we have used that $\ddot{\bar{\pi}} = 0$ and ignored $\mathcal{O}\left(\delta\dot{\pi}\right)^2$ terms. Eq. (5.11) has the same structure as a fluid with $w = 0$, which can be seen by multiplying both terms by $\frac{a^3}{a^3}$ to get a total time derivative,

$$\frac{2\dot{\bar{\pi}}}{a^3}\left[\frac{d}{dt}\left(a^3 H\delta\dot{\pi}\right)\right] = 0, \tag{5.12}$$

$$\delta\dot{\pi} = \frac{C'}{\dot{a}a^2}. \tag{5.13}$$

Recall Eq. (5.6) and Eq. (5.7),

$$\delta\dot{\pi} = C\left(1+w\right)t^{-\frac{1-w}{1+w}}, \tag{5.14}$$

with $C = \frac{3}{2a_0^3}C'$. And for,

$$-1 < w < 1, \tag{5.15}$$

the fluctuations of $\dot{\pi}$ will redshift away as the universe expands. And we have shown that our constant $\dot{\pi}$ tracking solution is an attractor under the Ω^{-2} approximation.

5.3 Stability

In this section, we study whether perturbations around the π solutions derived above are free of ghost-like instabilities, that is, whether perturbations have positive kinetic terms. Additionally, we will also verify that fluctuations have a real-valued sound speed. This analysis can, of course, be equally performed in either Einstein or Jordan frame. For concreteness, we choose to work in Einstein frame, since the kinetic term for metric and π fluctuations are diagonal in this frame. We only focus on perturbations in π, which is a valid approximation in the strong coupling regime $Hr_c \gg 1$. Indeed, in this limit the backreation of π on the metric is consistently small. The Einstein action given in Eq. (3.14) contains 3 terms in which instabilities could potentially arise,

$$3\beta^2(\partial\pi)^2,\ \Lambda^{-3}(\partial\pi)^2\Box\pi, \text{ and } 2\beta {M_{\rm pl}}^{-1}\Lambda^{-3}\left(\partial\pi\right)^4.$$

The term that dominates over the others is the non-linear term. This is as expected since the solutions of interest were derived in the strong coupling regime where non-linearities are important. To show this, we will only be concerned with orders of magnitude, and we will note that in each of our analytic solutions that $\dot{\pi}^2 \sim M_{\rm pl}\Lambda^3$.

$$\begin{aligned} 3\beta^2(\partial\pi)^2 &\sim M_{\rm pl}\Lambda^3, && (5.16)\\ \Lambda^{-3}(\partial\pi)^2\Box\pi &\sim M_{\rm pl}H\dot{\pi} \\ &\sim H\left(M_{\rm pl}\Lambda\right)^{\frac{3}{2}}, && (5.17)\\ 2\beta {M_{\rm pl}}^{-1}\Lambda^{-3}\left(\partial\pi\right)^4 &\sim M_{\rm pl}\Lambda^3. && (5.18) \end{aligned}$$

And the $3\beta^2(\partial\pi)^2$ and $2\beta {M_{\rm pl}}^{-1}\Lambda^{-3}\left(\partial\pi\right)^4$ terms are of the same order. Consequently, we only need to compare the $3\beta^2(\partial\pi)^2$ and $\Lambda^{-3}(\partial\pi)^2\Box\pi$ terms, which will compare

the $\Lambda^{-3}(\partial\pi)^2\Box\pi$ term to both terms,

$$\begin{aligned}\frac{\Lambda^{-3}(\partial\pi)^2\Box\pi}{3\beta^2(\partial\pi)^2} &\sim \frac{HM_{\rm pl}{}^{\frac{1}{2}}}{\Lambda^{\frac{3}{2}}} \\ &\sim Hr_c. \end{aligned} \tag{5.19}$$

For $Hr_c \gg 1$, the $\Lambda^{-3}(\partial\pi)^2\Box\pi$ term will dominate the other two terms. Accordingly, we analyze the stability of this term, by perturbing around $\pi = \overline{\pi} + \delta\pi$. Keeping only terms quadratic in perturbation we obtain,

$$\Lambda^{-3}(\partial\pi)^2\Box\pi_{(\delta\pi)^2} = \Lambda^{-3}\left(\partial\delta\pi\right)^2\Box\overline{\pi} + 2\Lambda^{-3}\nabla_\mu\overline{\pi}\nabla^\mu\delta\pi\Box\delta\pi. \tag{5.20}$$

Using integration by parts and noting that $\dot{\pi}$ is constant in all our solutions, one can obtain,

$$\Lambda^{-3}(\partial\pi)^2\Box\pi_{(\delta\pi)^2} = -6\Lambda^{-3}H\dot{\overline{\pi}}\left(\partial\delta\pi\right)^2. \tag{5.21}$$

In general, the equation of motion for π in the strong coupling regime is approximately invariant[2] under $\dot{\pi} \to -\dot{\pi}$, thus both signs are allowed. Clearly we have two branches of solutions from Eq. (5.21), depending on whether $\dot{\pi}$ is positive or negative. For stability, we require the sign on the kinetic term to be positive, otherwise the solution suffers from ghost instabilities. Then, by this analysis, the positive branch is unstable and the negative branch is stable. This is exactly the same structure that arises in DGP [20]!

Additionally, the speed of sound is manifestly real, another requirement of stability. We can easily see from Eq. (5.21), that $(\partial_0\delta\pi)^2$ and $\left(\vec{\nabla}\pi\right)^2$ have the same coefficient, which gives the speed of sound, $c_{\rm s} = 1$, just like fluctuations of normal scalar fields. In particular, perturbations in π do not cluster, but instead free-stream.

[2]For example, see Eq. (4.22).

We will now consider the stability of our analytic solutions. For the static solution, only Eq. (5.16) contributes to the quadratic lagrangian for perturbations, and it manifestly has the right sign. This is just the statement that perturbations around flat space are stable, and also is agrees with DGP. For the self-acclerating solution, we have Eq. (5.2) and Eq. (5.5). Substitution into Eq. (5.21) yields,

$$(\partial\pi)^2\Box\pi_{(\delta\pi)^2} = -\frac{8}{3}\beta^2\Lambda^3\left(\partial\delta\pi\right)^2. \tag{5.22}$$

We can clearly say that this solution is unstable, as the sign of the 2nd order perturbations is negative-definite. Again, this is precisely the same result as DGP, where our self-accelerating solution suffers from instability. Finally we analyze the constant $\dot{\pi}$ tracking solution, we have Eq. (5.10), with Hubble defined by Eq. (5.6) and Eq. (5.7). Then Eq. (5.21) becomes,

$$(\partial\pi)^2\Box\pi_{(\delta\pi)^2} = -\alpha\frac{4}{t\left(1+w\right)}\left(\frac{\beta M_{\rm pl}\Lambda^3}{3}\frac{1-3w}{1-w}\right)^{\frac{1}{2}}\left(\partial\delta\pi\right)^2. \tag{5.23}$$

As we said before, we have choice over the sign of the 2nd order perturbations. If we choose $\alpha = -1$ this branch will be stable, and $\alpha = +1$ will be the unstable branch. So, we choose $\alpha = -1$ and our constant $\dot{\pi}$ tracking solution is a stable, useful approximation of the π fluid evolution.

It must be noted that we have restricted our attention for this analysis to perturbative stability, by focusing on the quadratic lagrangian. It is nevertheless true that, even the "stable" branch is actually unstable under non-linear perturbations. In other words, it is possible that there exists other regions of solution space around which perturbations are unstable. However, as shown in [20], at least in the decoupling limit, the stable branch is stable non-linearly and classically disconnected from the unstable branch.

5.4 Constant $\dot{\pi}$ Tracking Solution Revisited

It appears that we have found a constant $\dot{\pi}$ solution branch which is stable. We wish to now check that π is a subdominant energy component at early times, in order to satisfy constraints on dark energy contributions at big bang nucleosynthesis and in the cosmic microwave background [1, 40]. To do so, we start with Eq. (4.12), and rearrange to determine the contribution,

$$\sum_i^n \rho_i = 3{M_{\rm pl}}^2 H^2 \left[1 + 2{M_{\rm pl}}^{-1} H^{-1} \dot{\pi} \left({M_{\rm pl}}^{-1} \Lambda^{-3} \dot{\pi}^2 - \beta\right)\right]. \tag{5.24}$$

Substitute Eq. (5.10),

$$\sum_i^n \rho_i = 3{M_{\rm pl}}^2 H^2 \left[1 - \frac{4\beta}{3\left(1-w\right)} {M_{\rm pl}}^{-1} H^{-1} \dot{\pi}\right], \tag{5.25}$$

noting that $\Lambda^3 = \frac{M_{\rm pl}}{r_c^2}$ and $\dot{\pi}^2 \sim M_{\rm pl}\Lambda^3$. Then $\dot{\pi} \sim \frac{M_{\rm pl}}{r_c}$ and,

$$\sum_i^n \rho_i = 3{M_{\rm pl}}^2 H^2 \left\{1 - 4\alpha \left[\frac{\beta}{3\left(1-w\right)}\right]^{\frac{3}{2}} \left(1-3w\right)^{\frac{1}{2}} \frac{1}{H r_c}\right\}. \tag{5.26}$$

For sufficiently large r_c we see that the correction is very small for early universe evolution ($H r_c \gg 1$). We are taking r_c to be of the order of the Hubble radius today, so early-time phenomenology is not affected by this solution.

We can additionally determine what the effective equation of state for this π field is. Recall Eq. (4.17) and substitute Eq. (5.10),

$$\begin{aligned} w_\pi &= -1 + \left(1 - \frac{\beta M_{\rm pl}}{\Lambda^{-3}\dot{\pi}^2}\right)^{-1} + \frac{2\beta^2\dot{\pi}}{3H}\left(\beta M_{\rm pl} - \Lambda^{-3}\dot{\pi}^2\right)^{-1} \\ &= -1 + \left(1 - \frac{3-3w}{1-3w}\right)^{-1} + \frac{2\beta\dot{\pi}}{3HM_{\rm pl}}\left(1 - \frac{1-3w}{3-3w}\right)^{-1} \\ &= \left(-\frac{3}{2} + \beta {M_{\rm pl}}^{-1} H^{-1}\dot{\pi}\right)\left(1-w\right). \end{aligned} \tag{5.27}$$

Again note that $\Lambda^3 = \frac{M_{\rm pl}}{r_c^2}$ and $\dot{\pi}^2 \sim M_{\rm pl}\Lambda^3$. Then $\dot{\pi} \sim \frac{M_{\rm pl}}{r_c}$ then,

$$w_\pi = -\frac{3}{2}(1-w) - \frac{\beta}{\sqrt{3}}\left[\beta(1-3w)(1-w)\right]^{\frac{1}{2}}\frac{1}{Hr_c}, \tag{5.28}$$

where we have used $\alpha = -1$ from the stability argument. For $\beta > 0$, $w_\pi \leq -1$ for all $w \leq \frac{1}{3}$. One should note that the $\frac{1}{Hr_c}$ also makes w_π even more negative, for late times. For $\beta < 0$ and early times ($Hr_c \gg 1$), $-1 \leq w_\pi < 0$ for all $\frac{1}{3} \leq w < 1$. For $\beta < 0$ and late times ($Hr_c \approx 1$), w_π can take on any value greater than -1, since β is variable. At w's limits, $\frac{1}{3}$ and 1, w_π must equal -1 and 0, respectively. It should be noted that the constant $\dot{\pi}$ tracking solution for $\beta < 0$ most likely breaks down at late times, since it requires $\frac{1}{3} \leq w < 1$.

From Eq. (4.14) we can also determine this solution's effect on the acceleration equation. Again using $\ddot{\pi} = 0$,

$$\frac{\ddot{a}}{a} = -\frac{H^2}{2}\left[\frac{1}{3{M_{\rm pl}}^2H^2}\left(\sum_i^n \rho_i + 3\sum_i^n p_i\right) + \frac{4\beta^2\dot{\pi}^2}{{M_{\rm pl}}^2H^2} - \frac{2\Lambda^{-3}\dot{\pi}^3}{{M_{\rm pl}}^2H} - \frac{4\beta\dot{\pi}}{M_{\rm pl}H}\right], \tag{5.29}$$

where we have inserted $\frac{H^2}{H^2}$ to compare $\frac{1}{3{M_{\rm pl}}^2H^2}\left(\sum_i^n \rho_i + 3\sum_i^n p_i\right)$, which is of order unity, to the correction due to π. This is given by,

$$\left(\frac{\ddot{a}}{a}\right)_\pi = \frac{4\beta^3\dot{\pi}^2}{{M_{\rm pl}}^2H^2} - \frac{2\Lambda^{-3}\dot{\pi}^3}{{M_{\rm pl}}^2H} - \frac{4\beta\dot{\pi}}{M_{\rm pl}H}. \tag{5.30}$$

Inserting Eq. (5.10) and $\alpha = -1$,

$$\left(\frac{\ddot{a}}{a}\right)_\pi = \frac{2\beta}{3\sqrt{3}}\left(\frac{7-9w}{1-w}\right)\left(\beta\frac{1-3w}{1-w}\right)^{\frac{1}{2}}\frac{1}{Hr_c} + \frac{4\beta^3}{3}\left(\frac{1}{Hr_c}\right)^2. \tag{5.31}$$

For $Hr_c \gg 1$, these are small corrections to early time cosmology, as expected. For $\beta > 0$ and late times, the π field will cause the universe to accelerate.

We now leave this analytical approximation and evolve the π field numerically.

Chapter 6

Numerical Results

In appears we have developed an effective 4d action which consistently reproduces many of the interesting features of DGP. We now numerically analyze this model for general functions of π to determine its cosmological implications. We expect an attracting branch of solutions corresponding to the choice of $\alpha = -1$, as we saw in chapter 5. We show this numerically, by finding that the constant $\dot{\pi}$ tracking solution is an attractor. This simultaneously shows that our $\Omega^{-2} \approx 1$ approximation is indeed consistent. Perhaps the most interesting aspect of this model is that it has an effective $w_\pi \leq -1$ for $w \leq \frac{1}{3}$. We show the effect this modification has on the $w_{\rm tot}$, the relative fluid densities, and the late-time behaviour of the universe. We additionally show that w_π tracks $w_{\rm tot}$, as we expect from the tracking solution (giving further weight to the claim that our approximation is consistent), and then place a rough constraint on r_c from WMAP5 data.

6.1 Linearized Equations

In this section, we linearize our equations in order to numerically integrate them. This is accomplished by defining new parameters which reduce our Friedmann equation, π equation of motion, and continuity equations to first order. We start with Eq. (4.9),

$$\frac{d}{dt}\left(H\dot{\pi}^2\right) + 3H^2\dot{\pi}^2 = \beta M_{\rm pl}\Lambda^3 H^2\left(\frac{H'}{H} + 2\right)\Omega^{-2}, \tag{6.1}$$

where $'$ denotes the derivative with respect to the e-folding time $N = \ln a$ (and $dN = Hdt$), and we have replaced R according to,

$$R = 6\left(\frac{\ddot{a}}{a} + \frac{\dot{a}^2}{a^2}\right) = 6\left(\dot{H} + H^2 + H^2\right) = 6H^2\left(\frac{H'}{H} + 2\right). \tag{6.2}$$

Define the following variables to linearize our equations,

$$\begin{aligned}
M_{\rm pl}\Lambda^3 q &\equiv \dot{\pi}^2, & (6.3)\\
\frac{H}{\tilde{H}} &\equiv 2\left(\frac{\Lambda^3}{M_{\rm pl}}\right)^{\frac{1}{2}}, & (6.4)\\
\lambda &\equiv e^{-2\beta {M_{\rm pl}}^{-1}\pi}, & (6.5)\\
z_i &\equiv \frac{\rho_i}{4M_{\rm pl}\Lambda^3\lambda\tilde{H}^2}. & (6.6)
\end{aligned}$$

And make note of the following implied relations,

$$\begin{aligned}
\pi' &= \frac{\alpha}{2}M_{\rm pl}\frac{q^{\frac{1}{2}}}{\tilde{H}}, & (6.7)\\
\ddot{\pi} &= \alpha\Lambda^3\tilde{H}\frac{q'}{q^{\frac{1}{2}}}, & (6.8)\\
\frac{H'}{H} &= \frac{\tilde{H}'}{\tilde{H}}, & (6.9)\\
\lambda' &= -\alpha\beta\lambda\frac{q^{\frac{1}{2}}}{\tilde{H}}. & (6.10)
\end{aligned}$$

Now, Eq. (6.1) becomes,

$$H^2 q' + H H' q + 3H^2 q = \beta\lambda H^2 \left(\frac{H'}{H} + 2\right), \tag{6.11}$$

$$q' = \frac{\tilde{H}'}{\tilde{H}} (\beta\lambda - q) + 2\beta\lambda - 3q. \tag{6.12}$$

And we have linearized the π equation of motion in terms of the variable q. Next, we take (4.12) and substitute our new variables,

$$\begin{aligned} 1 &= \frac{\sum_i^n \rho_i}{3{M_{\rm pl}}^2 H^2 \lambda} + \frac{2\dot{\pi}}{M_{\rm pl} H} \left(\beta - \frac{q}{\lambda}\right) \\ &= \alpha \frac{q^{\frac{1}{2}}}{\tilde{H}} \left(\beta - \frac{q}{\lambda}\right) + \frac{1}{3} \sum_i^n z_i. \end{aligned} \tag{6.13}$$

This is our linearized form of the Friedmann equation. We will use this a check in our numerical integration, to ensure that our variables are evolving correctly and satisfying our equations (i.e. that this combination of variables always equals 1, for each time step). Rearranging (6.13) we get

$$z_{\rm m} = 3 - z_{\rm r} - z_\Lambda + 3\alpha \frac{q^{\frac{1}{2}}}{\tilde{H}} \left(\frac{q}{\lambda} - \beta\right), \tag{6.14}$$

which is our linearized $\rho_{\rm m}$ equation. We can also determine our form of the continuity equation from Eq. (6.6),

$$\begin{aligned} \frac{z_i'}{z_i} &= \frac{\rho_i'}{\rho_i} - \frac{\lambda'}{\lambda} - \frac{2\tilde{H}'}{\tilde{H}} \\ &= \frac{1}{\tilde{H}} \left(\alpha\beta q^{\frac{1}{2}} - 2\tilde{H}'\right) - 3\left(1 + w_i\right), \end{aligned} \tag{6.15}$$

where we have used $\rho_i' = -3\left(1 + w_i\right)\rho_i$. The last remaining variable that we need to linearize is H, which we do so by taking the derivative of the Friedmann equation,

$$\frac{d}{dN}\left(\lambda\tilde{H}^2\right) = \frac{d}{dN}\left[\alpha\left(\beta\lambda - q\right)\tilde{H} q^{\frac{1}{2}} + \tilde{H}^2 \frac{\sum_i^n \rho_i}{3{M_{\rm pl}}^2 H^2}\right]. \tag{6.16}$$

One can massage Eq. (6.16), using Eq. (6.12), Eq. (6.14) and the definition of our variables, to obtain,

$$\tilde{H}' = \frac{2\alpha\lambda q^{\frac{3}{2}} - \tilde{H}\left(3q^2 - \beta\lambda q + 2\lambda^2\right) + 2\alpha\tilde{H}^2\lambda q^{\frac{1}{2}}\left(\frac{1}{3}z_r - z_\Lambda + 3\right)}{\left(q - \beta\lambda\right)^2 - 4\alpha\tilde{H}\lambda q^{\frac{1}{2}}}. \tag{6.17}$$

And given Eq. (6.10), Eq. (6.12), Eq. (6.15), and Eq. (6.17) we are now in the position to numerically integrate these functions, and determine the evolution of our model for general π.

6.2 Runge-Kutta Integration

Using the linearized equations derived in Section 6.1, we run a Runge-Kutta of the fourth order (rk4) integration. The actual code is included in Appendix B. The figures included on the following pages were generated based on that code.

We first show the attracting branch of solutions[1] in Fig. 6.1 - 6.3, corresponding to the choice of $\alpha = -1$. Each of these plots has a different initial condition for $\dot{\pi}$, perturbed by a term $\delta\dot{\pi}$. Fig. 6.1 is the unperturbed evolution, Fig. 6.2 has $\delta\dot{\pi} = 7\dot{\pi}_0$, and Fig. 6.3 has $\delta\dot{\pi} = 10\dot{\pi}_0$. Clearly, these plots also show that the constant $\dot{\pi}$ tracking solution is also an attractor, and thus our approximation in Chapter 5 was a consistent one. In particular, Fig. 6.3, clearly shows the general ρ_π evolution following the constant $\dot{\pi}$ tracking solution. It must be noted that in these figures, we are plotting $\log \rho_i$ vs. $1 + Z$, but $\rho_\pi < 0$, for $\alpha = -1$ (this is most easily seen from Eq. (4.15)). Thus, we are actually plotting $\alpha\rho_\pi$ to make contact with the evolution of the other fluid densities. This subtlety of the π field having an effective negative energy density will make for some interesting late-time dynamics, as well as, trick one's intuition about $w_\pi < -1$. Additionally note that the $\Omega^{-2} \approx 1$ is a good approximation all the way up to the present.

In next series of figures, Fig. 6.4 - 6.12, we show the effect r_c has on suppressing the π dynamics, a theme which has been discussed throughout this thesis[2]. Each series of plot will start first by showing, $r_c \sim 5 \times 10^{29}$ cm, then $r_c \sim 6 \times 10^{29}$ cm, and finally $r_c \sim 1 \times 10^{30}$ cm. Fig. 6.4 - 6.6 show the effect that π has on the density parameters Ω_i. Since $\rho_\pi < 0$ the π field density parameter will also be negative.

[1] These plots have $r_c \sim 5 \times 10^{29}$ cm.
[2] See Sections 2.1, 2.3, 3.3, and 5.4.

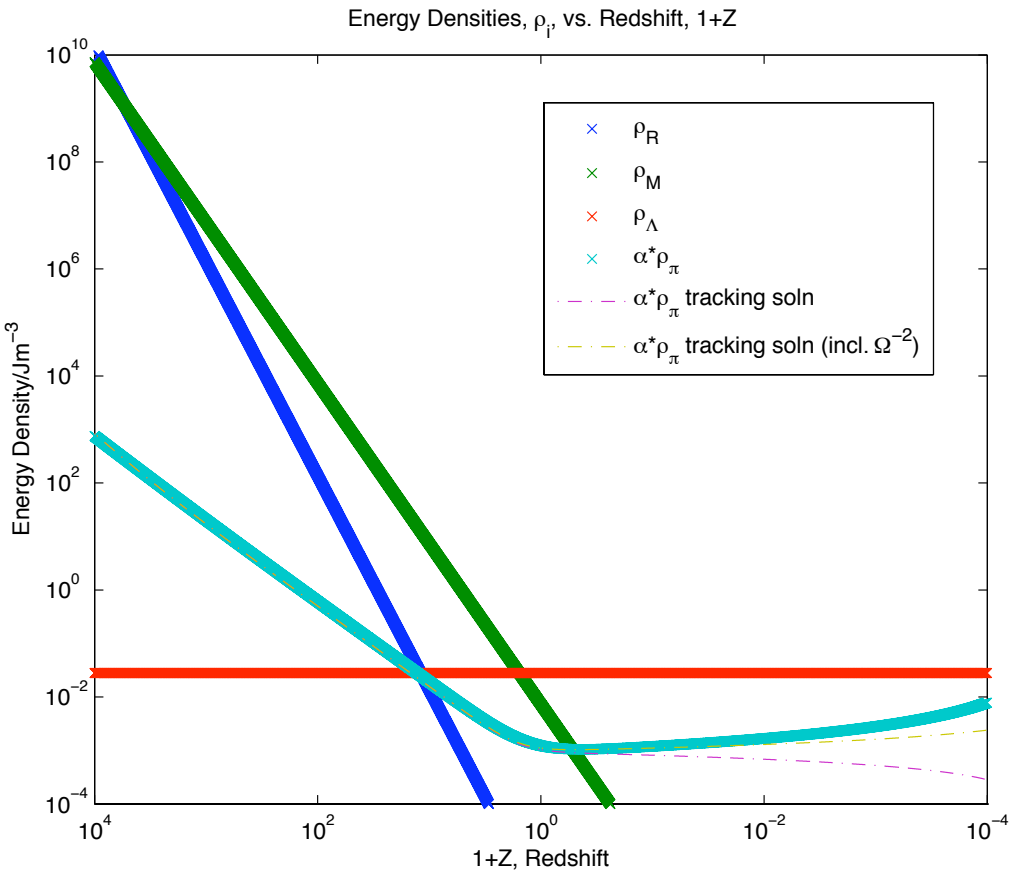

Figure 6.1: Stability of $\dot{\pi}$ tracking solution: $\delta\dot{\pi} = 0$

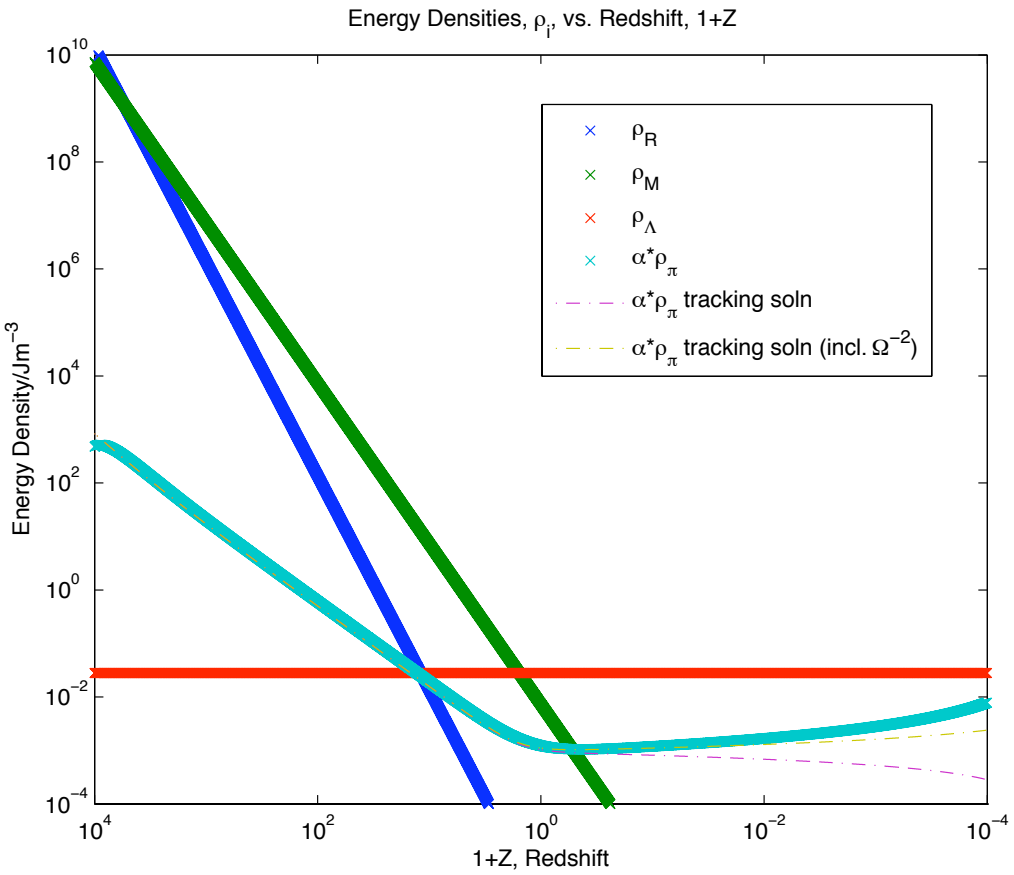

Figure 6.2: Stability of $\dot{\pi}$ tracking solution: $\delta\dot{\pi} = 7\dot{\pi}_0$

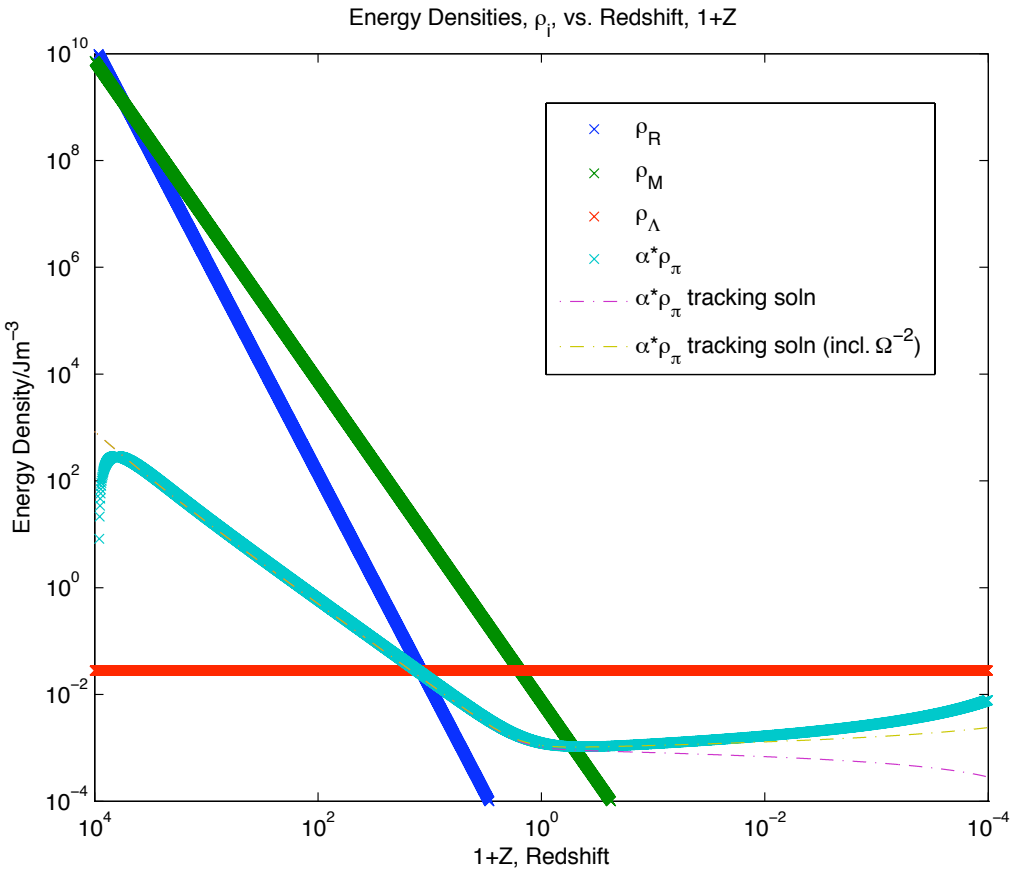

Figure 6.3: Stability of $\dot{\pi}$ tracking solution: $\delta\dot{\pi} = 10\dot{\pi}_0$

This means that as π grows, the other fluid components must have $\sum_{\text{not}\,\pi}^{n} \Omega_{\text{not}\,\pi} > 1$, since $\sum_i^n \Omega_i = 1$! This is dramatically shown in Fig. 6.4. We have also plotted the effective density parameter of the dark sector, namely the combination of Ω_π and Ω_Λ, and it limits to 1, as expected. Again, we must stress here that r_c dampens or enhances the effects of the π, as it defines the scale that at which gravity crosses over between 3+1-dimensional behaviour and 4+1-dimensional behaviour. These graphs show nicely that our model is completely consistent with the DGP picture. The higher r_c we choose, the further we suppress the π effect, and the longer it takes π to have an effect. It must be noted that the π is only suppressed, for $t \to \infty$, and π asymptotes to the same solution shown dramatically in Fig. 6.4, for any r_c.

We next move to the series of plots (Fig. 6.7 - 6.9) which show w_{tot} vs. $1 + Z$, for our model. An immediate property that is noticed, is that w_{tot} grows for late times! This seems completely at odds to the result derived in Eq. (5.28). For late times, we have only ρ_Λ and ρ_π. $w_\Lambda = -1$ and we have shown that $w_\pi < -1$ for all times, then how is $w_{\text{tot}} \not< -1$? This is where $\rho_\pi < 0$ causes very interesting dynamics, and tricks one's intuition. If we consider the late-time behaviour, with only ρ_Λ and ρ_π we have,

$$\begin{aligned} \dot{H} &= \sum_i^n -\frac{1}{2}\left(1 + w_i\right)\rho_i = -\frac{1}{2}\left(1 - 1\right)\rho_\Lambda - \frac{1}{2}\left(1 + w_\pi\right)\rho_\pi \\ &= -\frac{1}{2}\left(1 + w_\pi\right)\rho_\pi. \end{aligned} \tag{6.18}$$

Also recall, the continuity equation,

$$\dot{\rho}_\pi = -3H\left(1 + w_\pi\right)\rho_\pi. \tag{6.19}$$

and we have from before that $w_\pi < -1$, then $(1 + w_\pi) < 0$.

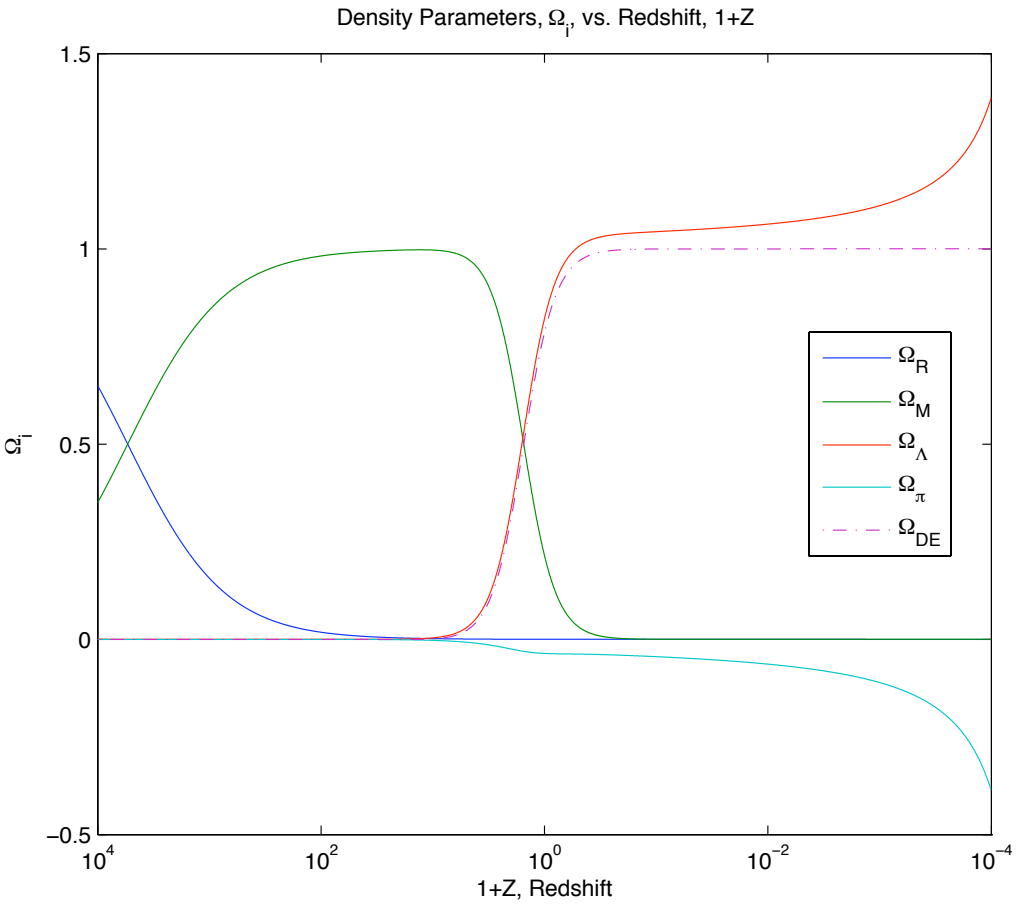

Figure 6.4: Ω_i vs. $1+Z$: $r_c \sim 5 \times 10^{29}$ cm

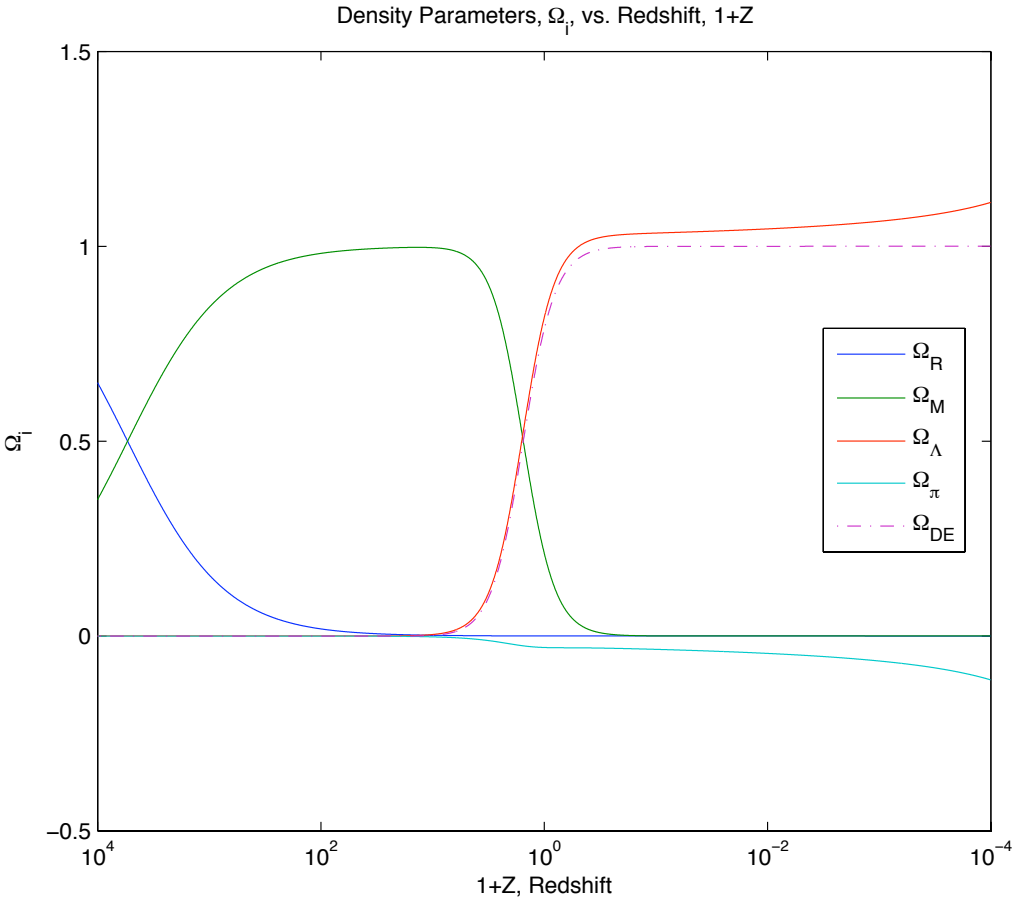

Figure 6.5: Ω_i vs. $1+Z$: $r_c \sim 6 \times 10^{29}$ cm

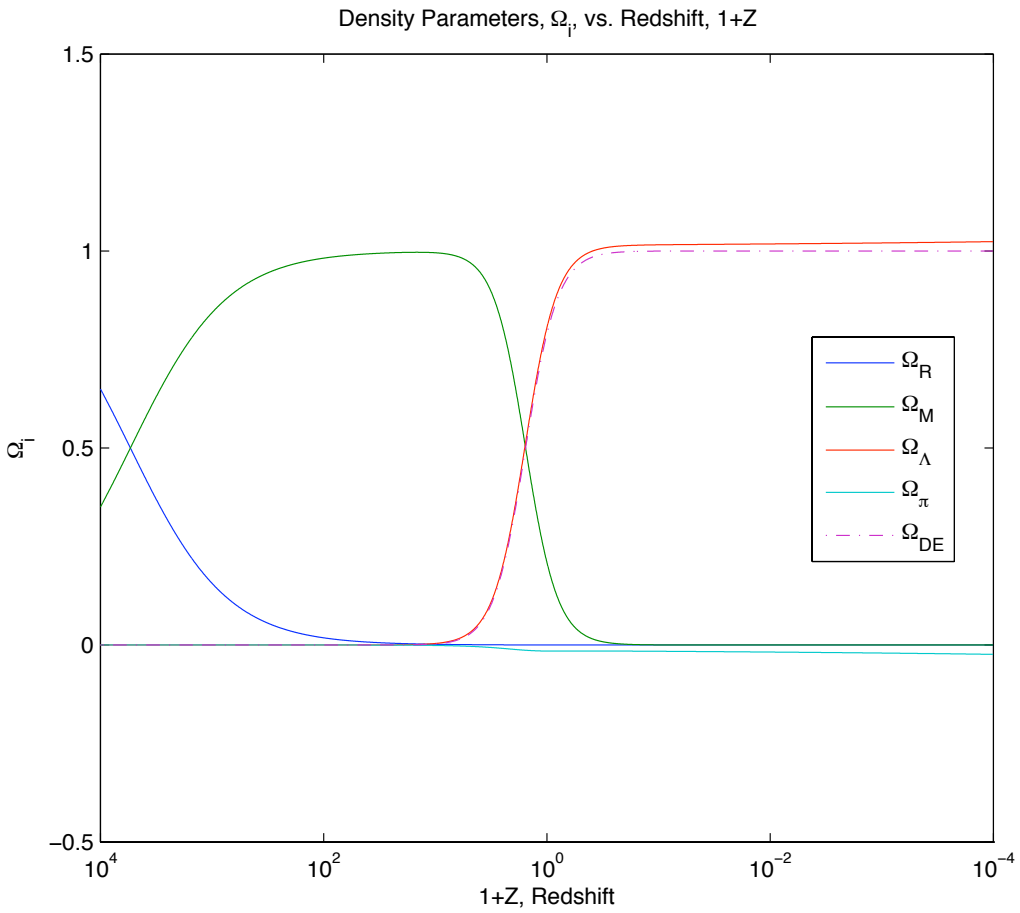

Figure 6.6: Ω_i vs. $1+Z$: $r_c \sim 1 \times 10^{30}$ cm

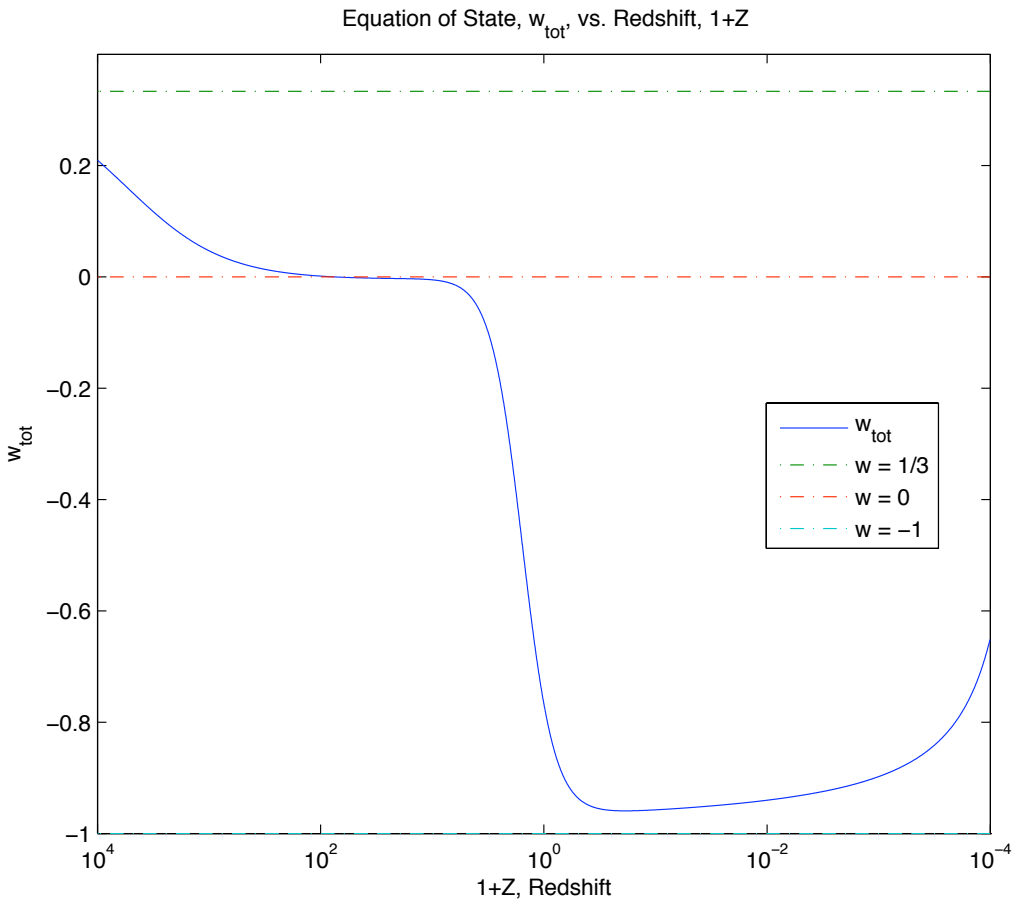

Figure 6.7: $w_{\rm tot}$ vs. $1+Z$: $r_c \sim 5 \times 10^{29}$ cm

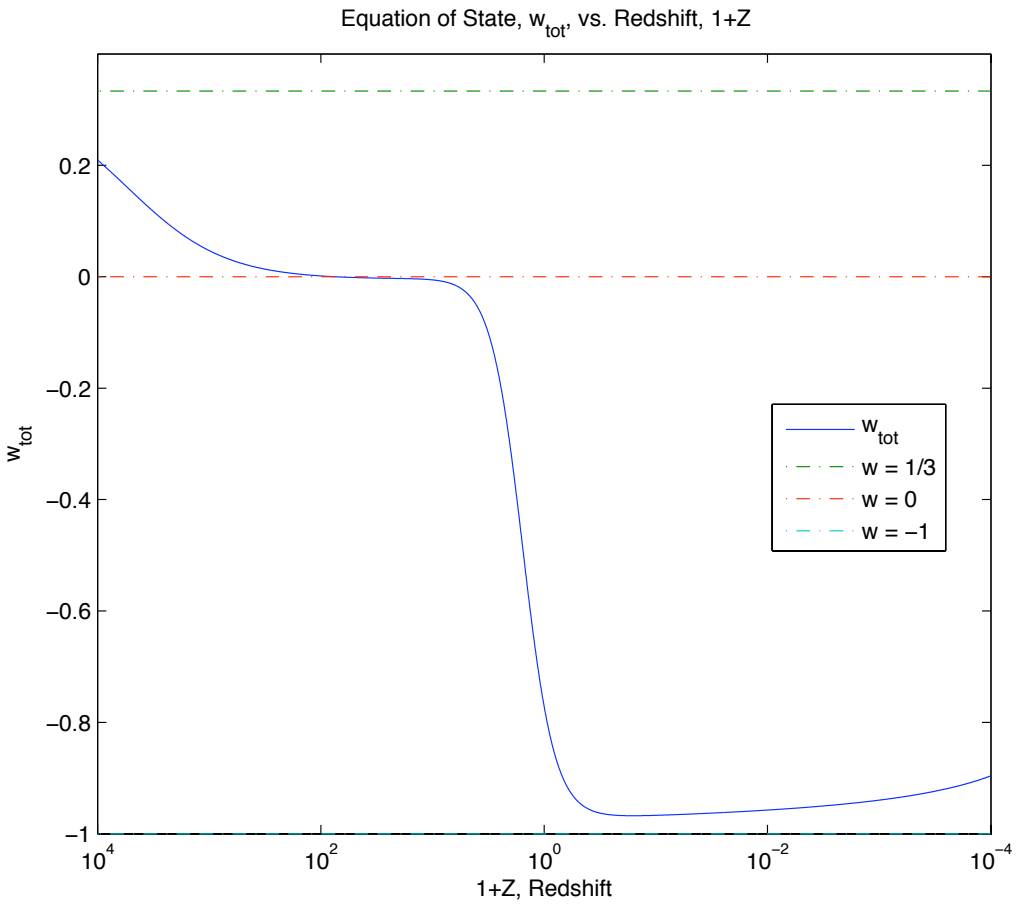

Figure 6.8: $w_{\rm tot}$ vs. $1+Z$: $r_c \sim 6 \times 10^{29}$ cm

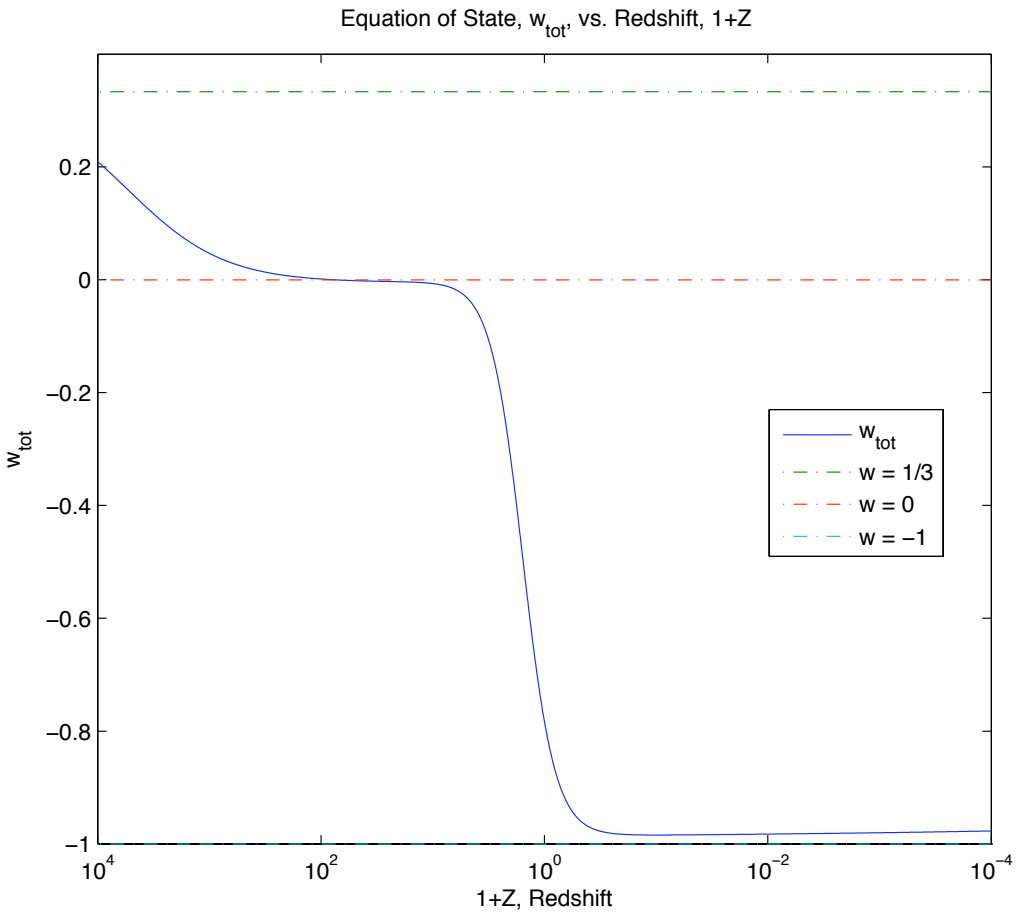

Figure 6.9: $w_{\rm tot}$ vs. $1+Z$: $r_c \sim 1 \times 10^{30}$ cm

This means that Eq. 6.19 has the following structure,

$$\dot{\rho}_\pi \sim +3H\rho_\pi, \tag{6.20}$$

where the R.H.S. coefficient is positive-definite. Then, $\dot{\rho}_\pi$ is always the same sign as ρ_π, hence, $|\rho_\pi|$ will always grow! We start with $\rho_\pi < 0$, then we will always have $\rho_\pi < 0$. Now if we consider this behaviour in Eq. (6.18), we see that $\dot{H}$ is indeed negative for $w_\pi < -1$. The dynamics, however, go further than that. As one can see from Fig. 6.7, it appears that the universe is heading for a contraction phase. This is precisely what this analysis expects, as ρ_π is becoming increasingly negative (w_π is also becoming increasingly negative). Then we have from Eq. (6.18), $\dot{H}$ also becoming increasingly negative. This is what you would expect for a fluid growing with positive density, exactly a contraction phase! So we see in this theory, that the late-time behaviour is that of a contracting universe, due to the π field, certainly something one would not immediately expect in an DGP effective model.

We now turn to the final three figures, Fig. 6.10 - 6.12. These show w_π as function of redshift. In particular, we are showing that w_π does indeed track $w_{\rm tot}$, as we analytically showed for the constant $\dot{\pi}$ solution. We include these plots add further weight to the claim that our approximation in Chapter 5 is completely consistent. Notice that during matter domination, w_π is indistinguishable from the expected w_π of the tracking solution, and equals $-\frac{3}{2}$ as expected. There is one additional thing to note about these last figures, at very late times, it appears that w_π and the expected w_π from the tracking solution have completely different behaviours. Indeed, at very late times the $\Omega^{-2} \approx 1$ approximation does eventually break down[3].

[3]The timescale is, of course, dependent on r_c.

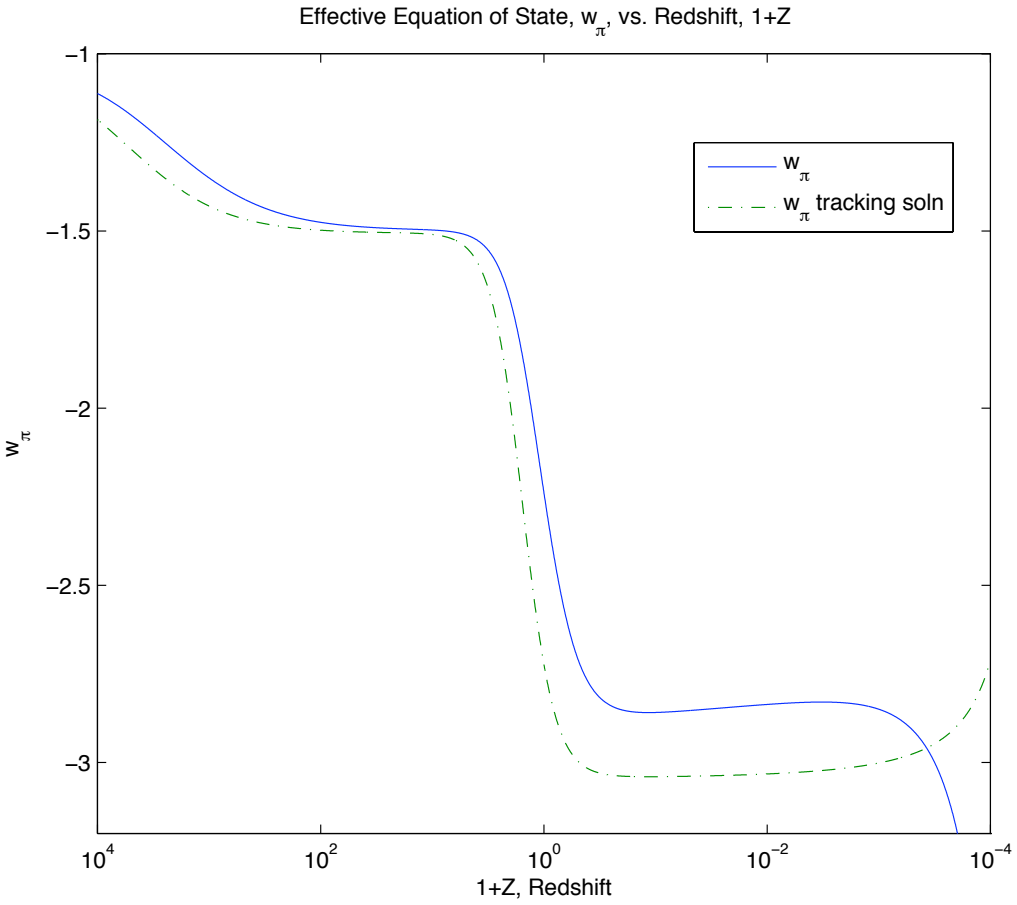

Figure 6.10: Effective equation of state, w_π vs. $1+Z$: $r_c \sim 5 \times 10^{29}$ cm

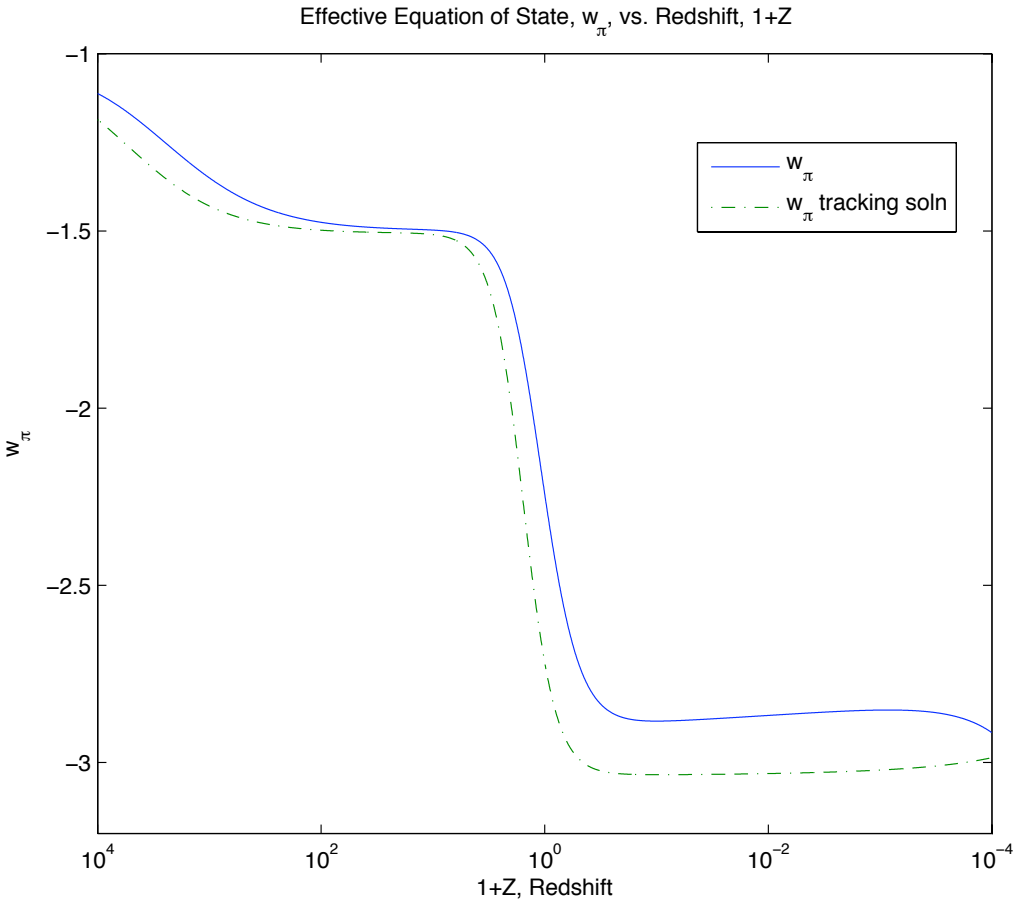

Figure 6.11: Effective equation of state, w_π vs. $1+Z$: $r_c \sim 6 \times 10^{29}$ cm

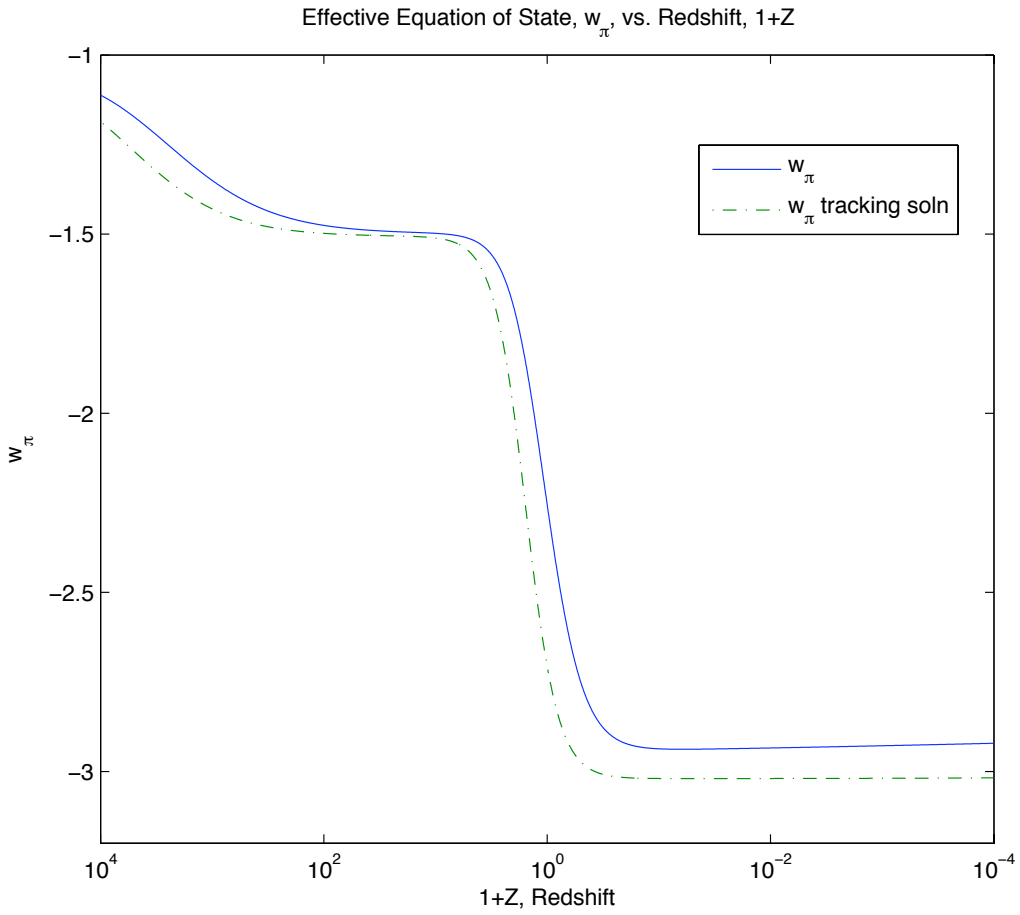

Figure 6.12: Effective equation of state, w_π vs. $1 + Z$: $r_c \sim 1 \times 10^{30}$ cm

We will clarify this issue as follows; w_π becomes increasingly negative for late times, but as we saw in the previous series of graphs, this causes $w_{\rm tot}$ to increase. Since w_π of the tracking solution only tracks $w_{\rm tot}$ and neglects Ω^{-2}, it increases as well. The discrepancy is doubly enhanced, since w_π becoming more negative is driving the constant $\dot{\pi}$ equation of state positively.

We will now end this numerical analysis by placing a rough constraint on r_c. Clearly for an r_c too small, we will see unwanted deviations from the observed cosmological history, since π has an increasingly earlier effect. To constrain r_c we fix $\Omega_{\rm DE}$ to 0.736 today (the maximum likelihood value from WMAP5 [1]). From this, we vary r_c until we at the maximum allowed value of w today, which is -0.932 (also from WMAP5). This places a bound on $r_c \geq 5 \times 10^{29}$ cm. This bound on r_c is an order of magnitude greater than previous older bounds. Correspondingly, our bound gives a maximum anomalous perihelion precession of the moon $\sim 1 \times 10^{-13}$. This is two orders of magnitude below current experiments, and one order of magnitude below upcoming experiments [10, 36]. This constraint on r_c is admittedly a rough estimate. Our methodology was coarse on many levels. First, we should not fix $\omega_{\rm DE}$ and then allow w to vary based on r_c. Instead, we should allow both parameters to vary. Second, the constraint on w we use assumes constant w, which is of course not valid in our case. To do a careful job we should repeat the entire likelihood analysis within our context, but this is something which has been left for future analysis.

Chapter 7

Discussions and Outlook

Cosmic acceleration requires an explanation. While the currently accepted model uses vacuum energy as that explanation, it may be the case that Einstein's theory of gravity is becoming unreliable at the bounds of our observations. It behooves us to then, develop a new model of gravity which is consistent with Einstein gravity, but modifies it at large distances. The Dvali-Gabadadze-Porrati model is a rare example of such a consistent infrared modification. It is, however notoriously difficult to study cosmology in, which further motivates one to find a simple 4d effective model which captures its phenomenology over a large range of physical regimes. In this thesis, we have developed such a model.

Our 4d effective theory encapsulates many of DGP's key features in a simple π action. As is the case with DGP, our Friedmann equation allows two branches of solutions, depending on the sign of the velocity of π. One branch corresponds to self-acceleration, and the other is asymptotically flat. The π field contributes an effective energy density to the Friedmann equation on the stable (unstable) branch which has

an effective equation of state $w < -1$ ($w > -1$).

Furthermore, the π field displays a cosmological analogue of the Vainshtein effect. In the presence of a background fluid, such as matter or radiation, the π dynamics are dominated by its non-linear interactions at early times ($Hr_c \gg 1$); the resulting effective energy density is then suppressed compared to the background fluid. In this regime where the π field is subdominant, we have analytically derived a tracking solution in which $\dot{\pi}$ is constant. We have shown that it is an attractor, since small perturbations redshift away. We have checked numerically the existence of this tracking solution and its attractor property and determined the effect on the total equation of state $w_{\rm tot}$. The late-time dynamics of universes which follow this model will go through a contraction phase, due to the π field. Additionally, it has been shown that w_π tracks $w_{\rm tot}$ for the majority of the evolution. Finally, from WMAP5 constraints on Ω_Λ and $w_{\rm DE}$, we have placed a rough (yet, stronger) constraint on $r_c \geq 10^{29}$ cm.

There are two immediate avenues which should be explored in this model; The calculation of luminosity-distance as function of redshift, which would place a stronger, and more accurate constraint on r_c; And the consequences on structure formation due to cosmological perturbations in this model. Some work should also be done analyzing the model general combination of functions which do not have $n > 2$ higher order derivatives.

APPENDIX

A. General $A(X)$ and $B(X)$

We will derive the π-EOM and field equations for a general $A(X)$ and $B(X)$ Einstein action. So, we start with the generalized NR action,

$$S_{GNR} = \int d^4x\sqrt{-g}\left[A(X) + B(X)\Box\pi\right]. \tag{A.1}$$

The π-EOM is,

$$\begin{aligned} 2\nabla_\nu\pi\nabla_\mu\nabla^\nu\left[\frac{d^2A}{dX^2}\nabla^\nu\pi + \frac{d^2B}{dX^2}\left(\nabla^\nu\pi\Box\pi - \nabla^\alpha\pi\nabla^\mu\nabla_\alpha\pi\right)\right] \\ +\frac{dA}{dX}\Box\pi + \frac{dB}{dX}\left[(\Box\pi)^2 - (\nabla_\mu\nabla_\nu\pi)^2 - \nabla^\mu\pi R^\beta_\mu\nabla_\beta\pi\right] &= -\frac{T^{(m)}_{\mathcal{E}}}{2}, \end{aligned} \tag{A.2}$$

where we have used $\nabla_\mu\Box\pi - \Box\nabla_\mu\pi = -R^\beta_\mu\nabla_\beta\pi$. Varying with respect to the metric gives,

$$\begin{aligned} T_{\mu\nu} &= 2\frac{dA}{dX}\nabla_\mu\pi\nabla_\nu\pi - g_{\mu\nu}A(X) \\ &\quad +\frac{dB}{dX}\left[2\nabla_\mu\pi\nabla_\nu\pi\Box\pi + g_{\mu\nu}\nabla_\alpha\pi\partial^\alpha(\partial\pi)^2 - \nabla_{(\mu}\pi\nabla_{\nu)}(\partial\pi)^2\right], \end{aligned} \tag{A.3}$$

as our stress-energy tensor. We can now assume an FRW background and that π is only a function of time. Let's calculate T_{00} and T_{ii},

$$T_{00} = 2\dot\pi\left(\frac{dA}{dX}\dot\pi - 3H\frac{dB}{dX}\dot\pi^2\right) + A(X), \tag{A.4}$$

$$T_{ii} = -A(X) + 2\frac{dB}{dX}\ddot\pi\dot\pi^2. \tag{A.5}$$

We can alternatively consider the following form of (A.2),

$$2\nabla_\mu\left[-\frac{dA}{dX}\nabla^\mu\pi + \frac{dB}{dX}\left(\nabla_\alpha\pi\nabla^\mu\nabla^\alpha\pi - \nabla^\mu\pi\Box\pi\right)\right] = T^{(m)}_{\mathcal{E}}, \tag{A.6}$$

and identify j^μ as,

$$-2\frac{dA}{dX}\nabla^\mu\pi + 2\frac{dB}{dX}\left(\nabla_\alpha\pi\nabla^\mu\nabla^\alpha\pi - \nabla^\mu\pi\Box\pi\right). \tag{A.7}$$

Using the identity, $\nabla_\mu j^\mu = \frac{1}{\sqrt{-g}}\partial_\mu\left(\sqrt{-g}j^\mu\right)$ for $T^{(m)}_{\mathcal{E}} = 0$, and $\sqrt{-g} = a^3$ and π only a function of time,

$$\partial_t\left\{a^3\left[2\frac{dA}{dX}\dot{\pi} + 2\frac{dB}{dX}\left(-3H\dot{\pi}^2\right)\right]\right\} = 0, \tag{A.8}$$

$$\frac{dA}{dX}\dot{\pi} - 3H\frac{dB}{dX}\dot{\pi}^2 = \frac{C}{a^3}. \tag{A.9}$$

This reduces T_{00} considerably for $T^{(m)}_{\mathcal{E}} = 0$,

$$T_{00} = \frac{C}{2a^3} + A(X). \tag{A.10}$$

From (A.8), we can solve for $\dot{\pi}$,

$$\dot{\pi} = \frac{\frac{dA}{dX} \pm \sqrt{\left(\frac{dA}{dX}\right)^2 + 12H\frac{dB}{dX}\left(\frac{C}{a^3}\right)}}{6H\frac{dB}{dX}}. \tag{A.11}$$

for $T^{(m)}_{\mathcal{E}} = 0$.

B. rk4 Integration Matlab Code

The following code was run in Matlab to numerically integrate our equations, to evolve our associated cosmology.

```
%%%%%%%%%%%%%%%%%%%%%%%%%%%%%%%%%%%%%%%%%%%%%%%%%
%                                               %
%   Nathan Chow                                 %
%                                               %
%   Modified Gravity - Effective DGP Code       %
%   matter, radiation, cosmological constant,   %
%   and pi field                                %
%                                               %
%   rk4 integration                             %
%                                               %
%   M.Sc - Sept. 2007 - December 2008           %
%                                               %
%%%%%%%%%%%%%%%%%%%%%%%%%%%%%%%%%%%%%%%%%%%%%%%%%

clear;

%set display to most decimal places (15)
format long g

%specify general variables, i.e. Ca = 3
```

```
al = -1;

ep = 1;

Mpl = 1;

Ca = 3;

Cb = 1e63;

Cbtil = 20;


%specify equation of state parameters

wr = 1/3;

wm = 0;

wl = -1;


%N runs from N_i = -4 to N_f = 4, with 3000 steps

stepsize = 3000;

Ai = 1e-4;

Af = 1e4;

N = linspace(log(Ai),log(Af),stepsize);


%set initial conditions

hubtil(1) = 1.58e5;

hubble(1) = 2*((Mpl*Cb)^(-1/2))*((Ca/3)^0.75)*hubtil(1);

hubtil(1) = hubtil(1)*Cbtil;

lambda(1) = 0.99;
```

```
pidot(1) = 1e-32;

q(1) = (Cb/Mpl)*((3/Ca)^0.5)*(pidot(1)^2);

BenchQ = al*((q(1)^0.5)/hubtil(1))*(ep - q(1)/lambda(1));
BenchR = 0.995;
BenchM = 0.99999999999 - BenchR - BenchQ;
BenchL = 1 - BenchR - BenchM - BenchQ;

zr(1) = 3*BenchR;
zm(1) = 3*BenchM;
zl(1) = 3*BenchL;

pidotconst(1) = (al*(((Mpl/Cb)*((Ca/3)^0.5)*q(1))^(0.5)))/(Cbtil^2);

%rk4 integration
for j = 1:(stepsize - 1);
    %output which stepsize it's currently on
    fprintf('step %d of %d\n',j,stepsize-1);

    %we use the friedmann equation as a check that everything is
    %evolving correctly
    check(j) = al*((q(j)^0.5)/hubtil(j))*(ep - q(j)/lambda(j))
    + (1/3)*(zm(j) + zr(j) + zl(j));
```

```
%width of stepsize
h(j) = N(j+1) - N(j);


%rk4 a values
ahubtil(j)= (2*al*lambda(j)*(q(j)^1.5) - hubtil(j)*(3*(q(j)^2)
- ep*lambda(j)*q(j) + 2*(lambda(j)^2))
+ 2*al*(hubtil(j)^2)*lambda(j)*(q(j)^0.5)*((1/3)*zr(j) - zl(j)
+ 3))/((q(j) - ep*lambda(j))^2 - 4*al*hubtil(j)*lambda(j)
*(q(j)^0.5));
aq(j) = (ahubtil(j)/hubtil(j))*(ep*lambda(j) - q(j))
+ 2*ep*lambda(j) - 3*q(j);
alambda(j) = -al*ep*lambda(j)*(q(j)^0.5)/hubtil(j);
azr(j) = ((1/hubtil(j))*(al*ep*(q(j)^0.5) - 2*ahubtil(j))
- 3*(1 + wr))*zr(j);
azm(j) = ((1/hubtil(j))*(al*ep*(q(j)^0.5) - 2*ahubtil(j))
- 3*(1 + wm))*zm(j);
azl(j) = ((1/hubtil(j))*(al*ep*(q(j)^0.5) - 2*ahubtil(j))
- 3*(1 + wl))*zl(j);


%rk4 b values
bhubtil(j)= (2*al*(lambda(j) + (h(j)/2)*alambda(j))*((q(j)
+ (h(j)/2)*aq(j))^1.5) - (hubtil(j) + (h(j)/2)*ahubtil(j))
*(3*((q(j)     + (h(j)/2)*aq(j))^2) - ep*(lambda(j) + (h(j)/2)
```

```
*alambda(j))    *(q(j) + (h(j)/2)*aq(j)) + 2*((lambda(j)
+ (h(j)/2)    *alambda(j))^2)) + 2*al*((hubtil(j) + (h(j)/2)
*ahubtil(j))^2)    *(lambda(j) + (h(j)/2)*alambda(j))
*((q(j) + (h(j)/2)*aq(j))^0.5)    *((1/3)*(zr(j) + (h(j)/2)
*azr(j)) - (zl(j) + (h(j)/2)*azl(j)) + 3))    /(((q(j) + (h(j)/2)
*aq(j)) - ep*(lambda(j) + (h(j)/2)    *alambda(j)))^2
- 4*al*(hubtil(j) + (h(j)/2)*ahubtil(j))*(lambda(j)
+ (h(j)/2)*alambda(j))*((q(j) + (h(j)/2)*aq(j))^0.5));
bq(j) = (bhubtil(j)/(hubtil(j) + (h(j)/2)*ahubtil(j)))
*(ep*(lambda(j) + (h(j)/2)*alambda(j)) - (q(j) + (h(j)/2)
*aq(j))) + 2*ep*(lambda(j) + (h(j)/2)*alambda(j))
- 3*(q(j) + (h(j)/2)*aq(j));
blambda(j) = -al*ep*(lambda(j) + (h(j)/2)*alambda(j))
*((q(j) + (h(j)/2)*aq(j))^0.5)/(hubtil(j)
+ (h(j)/2)*ahubtil(j));
bzr(j) = ((1/(hubtil(j) + (h(j)/2)*ahubtil(j)))
*(al*ep*((q(j) + (h(j)/2)*aq(j))^0.5) - 2*bhubtil(j))
- 3*(1 + wr))*(zr(j) + (h(j)/2)*azr(j));
bzm(j) = ((1/(hubtil(j) + (h(j)/2)*ahubtil(j)))
*(al*ep*((q(j) + (h(j)/2)*aq(j))^0.5) - 2*bhubtil(j))
- 3*(1 + wm))*(zm(j) + (h(j)/2)*azm(j));
bzl(j) = ((1/(hubtil(j) + (h(j)/2)*ahubtil(j)))
*(al*ep*((q(j) + (h(j)/2)*aq(j))^0.5) - 2*bhubtil(j))
- 3*(1 + wl))*(zl(j) + (h(j)/2)*azl(j));
```

```
%rk4 c values
chubtil(j)= (2*al*(lambda(j) + (h(j)/2)*blambda(j))*((q(j)
+ (h(j)/2)*bq(j))^1.5) - (hubtil(j) + (h(j)/2)*bhubtil(j))
*(3*((q(j) + (h(j)/2)*bq(j))^2) - ep*(lambda(j) + (h(j)/2)
*blambda(j))*(q(j) + (h(j)/2)*bq(j)) + 2*((lambda(j)
+ (h(j)/2)*blambda(j))^2)) + 2*al*((hubtil(j) + (h(j)/2)
*bhubtil(j))^2)*(lambda(j) + (h(j)/2)*blambda(j))
*((q(j) + (h(j)/2)*bq(j))^0.5)*((1/3)*(zr(j) + (h(j)/2)
*bzr(j)) - (zl(j) + (h(j)/2)*bzl(j)) + 3))/(((q(j) + (h(j)/2)
*bq(j)) - ep*(lambda(j) + (h(j)/2)*blambda(j)))^2
- 4*al*(hubtil(j) + (h(j)/2)*bhubtil(j))*(lambda(j)
+ (h(j)/2)*blambda(j))*((q(j) + (h(j)/2)*bq(j))^0.5));
cq(j) = (chubtil(j)/(hubtil(j) + (h(j)/2)*bhubtil(j)))
*(ep*(lambda(j) + (h(j)/2)*blambda(j)) - (q(j) + (h(j)/2)
*bq(j))) + 2*ep*(lambda(j) + (h(j)/2)*blambda(j))
- 3*(q(j) + (h(j)/2)*bq(j));
clambda(j) = -al*ep*(lambda(j) + (h(j)/2)*blambda(j))
*((q(j) + (h(j)/2)*bq(j))^0.5)/(hubtil(j)
+ (h(j)/2)*bhubtil(j));
czr(j) = ((1/(hubtil(j) + (h(j)/2)*bhubtil(j)))
*(al*ep*((q(j) + (h(j)/2)*bq(j))^0.5) - 2*chubtil(j))
- 3*(1 + wr))*(zr(j) + (h(j)/2)*bzr(j));
czm(j) = ((1/(hubtil(j) + (h(j)/2)*bhubtil(j)))
```

```
*(al*ep*((q(j) + (h(j)/2)*bq(j))^0.5) - 2*chubtil(j))
- 3*(1 + wm))*(zm(j) + (h(j)/2)*bzm(j));
czl(j) = ((1/(hubtil(j) + (h(j)/2)*bhubtil(j)))
*(al*ep*((q(j) + (h(j)/2)*bq(j))^0.5) - 2*chubtil(j))
- 3*(1 + wl))*(zl(j) + (h(j)/2)*bzl(j));

%rk4 d values
dhubtil(j)= (2*al*(lambda(j) + h(j)*clambda(j))*((q(j)
+ h(j)*cq(j))^1.5) - (hubtil(j) + h(j)*chubtil(j))
*(3*((q(j) + h(j)*cq(j))^2) - ep*(lambda(j) + h(j)
*clambda(j))*(q(j) + h(j)*cq(j)) + 2*((lambda(j)
+ h(j)*clambda(j))^2)) + 2*al*((hubtil(j) + h(j)
*chubtil(j))^2)*(lambda(j) + h(j)*clambda(j))*((q(j)
+ h(j)*cq(j))^0.5)*((1/3)*(zr(j) + h(j)*czr(j)) - (zl(j)
+ h(j)*czl(j)) + 3))/(((q(j) + h(j)*cq(j)) - ep
*(lambda(j) + h(j)*clambda(j)))^2 - 4*al*(hubtil(j)
+ h(j)*chubtil(j))*(lambda(j) + h(j)*clambda(j))
*((q(j) + h(j)*cq(j))^0.5));
dq(j) = (chubtil(j)/(hubtil(j) + h(j)*chubtil(j)))
*(ep*(lambda(j) + h(j)*clambda(j)) - (q(j) + h(j)
*cq(j))) + 2*ep*(lambda(j) + h(j)*clambda(j))
- 3*(q(j) + h(j)*cq(j));
dlambda(j) = -al*ep*(lambda(j) + h(j)*clambda(j))
*((q(j) + h(j)*cq(j))^0.5)/(hubtil(j) + h(j)*chubtil(j));
```

```
dzr(j) = ((1/(hubtil(j) + h(j)*chubtil(j)))*(al*ep*((q(j)
+ h(j)*cq(j))^0.5) - 2*dhubtil(j)) - 3*(1 + wr))
*(zr(j) + h(j)*czr(j));
dzm(j) = ((1/(hubtil(j) + h(j)*chubtil(j)))*(al*ep*((q(j)
+ h(j)*cq(j))^0.5) - 2*dhubtil(j)) - 3*(1 + wm))
*(zm(j) + h(j)*czm(j));
dzl(j) = ((1/(hubtil(j) + h(j)*chubtil(j)))*(al*ep*((q(j)
+ h(j)*cq(j))^0.5) - 2*dhubtil(j)) - 3*(1 + wl))
*(zl(j) + h(j)*czl(j));

%calculate the rk4 weighted change in
%each variable
changehubtil(j) = (h(j)/6)*(ahubtil(j) + 2*bhubtil(j)
+ 2*chubtil(j) + dhubtil(j));
changeq(j) = (h(j)/6)*(aq(j) + 2*bq(j) + 2*cq(j) + dq(j));
changelambda(j) = (h(j)/6)*(alambda(j)
+ 2*blambda(j) + 2*clambda(j) + dlambda(j));
changezr(j) = (h(j)/6)*(azr(j) + 2*bzr(j) + 2*czr(j) + dzr(j));
changezm(j) = (h(j)/6)*(azm(j) + 2*bzm(j) + 2*czm(j) + dzm(j));
changezl(j) = (h(j)/6)*(azl(j) + 2*bzl(j) + 2*czl(j) + dzl(j));

%step each variable
hubtil(j+1) = hubtil(j) + changehubtil(j);
q(j+1) = q(j) + changeq(j);
```

```
zr(j+1) = zr(j) + changezr(j);

zm(j+1) = zm(j) + changezm(j);

zl(j+1) = zl(j) + changezl(j);

lambda(j+1) = lambda(j) + changelambda(j);


%calculate pidot and hubble based on the

%linearized variables

pidot(j) = al*(((Mpl/Cb)*((Ca/3)^0.5)*q(j))^(0.5));

hubble(j) = 2*((Mpl*Cb)^(-1/2))

*((Ca/3)^0.75)*hubtil(j);


%as well as rho_pi, rho_m, rho_r, rho_l

rhopi(j) = 12*lambda(j)*(hubtil(j)^2)/(Cbtil^2)

*(Mpl/Cb)*((Ca/3)^(3/2))*al*((q(j)^0.5)/hubtil(j))

*(ep - q(j)/lambda(j));

rhor(j) = 4*lambda(j)*(hubtil(j)^2)/(Cbtil^2)

*(Mpl/Cb)*((Ca/3)^(3/2))*zr(j);

rhom(j) = 4*lambda(j)*(hubtil(j)^2)/(Cbtil^2)

*(Mpl/Cb)*((Ca/3)^(3/2))*zm(j);

rhol(j) = 4*lambda(j)*(hubtil(j)^2)/(Cbtil^2)

*(Mpl/Cb)*((Ca/3)^(3/2))*zl(j);


zpi(j) = al*((q(j)^0.5)/hubtil(j))

*(ep - q(j)/lambda(j));
```

```
%we will plot in terms of redshift
Z(j) = exp((-N(j))) - 1;

%the equation of state at each time
wtot(j) = -(2/3)*changehubtil(j)/(h(j)*hubtil(j)) - 1;

%plot our tracking solution
rhopiconst(j) = (-6)*Cb*hubble(j)
*(pidotconst(1)^3) + 6*ep*hubble(j)*Mpl
*lambda(j)*((Ca/3)^(1/2))*pidotconst(1);

%in some runs, the tracking solution breaks down
%(because of the lambda factor) so we set its
%value to zero, in the regime it breaks down
if al*rhopiconst(j) < 0;
    rhopiconst(j) = 0;
end

%plot standard slope to compare plots with
slope3rd(j) = 1/3;
slope0th(j) = 0;
slopeminus1(j) = -1;
slope0(j) = 0.55e-30;
```

```
    slope15(j) = (hubble(1)*(1+Z(j))^(1.5))*2.45e-7;
    slope2(j) = (hubble(1)*(1+Z(j))^(2))*1e-8;
    slope3(j) = (rhom(1)*(1+Z(j))^3)*1e-12;
    slope4(j) = (rhor(1)*(1+Z(j))^4)*1e-16;
end

%plot the energy density of the fluids vs. redshift, include
%standard slope = -4, -3 lines, as well as the rho_pi = const.
%tracking sol'n
figure
loglog(1+Z,rhom,'+',1+Z,rhor,'x',1+Z,rhol,'x',1+Z,
al*rhopi,'x',1+Z,slope3,'-',1+Z,slope4,'-',1+Z,
al*rhopiconst,'-');
ylim([1e-68 1e-50])
set(gca,'XDir','reverse');

%plot hubble vs. redshift, and slope = 2, 3/2, 0
figure
loglog(1+Z,hubble,'+',1+Z,slope2,'-',1+Z,
slope15,'-',1+Z,slope0,'-');
ylim([1e-32 1e-26])
set(gca,'XDir','reverse');

%plot the equation of state vs. redshift, and wtot = 1/3, 0, -1
```

```
figure
semilogx(1+Z,wtot,'x',1+Z,slope3rd,'-',1+Z,
slope0th,'-',1+Z,slopeminus1,'-');
ylim([-1.5 0.5])
set(gca,'XDir','reverse');
Z(stepsize) = Z(stepsize-1);
zpi(stepsize) = zpi(stepsize-1);

%plot the density parameter of the fluids vs. redshift
figure
semilogx(1+Z,zr/3,'+',1+Z,zm/3,'-',1+Z,zl/3,'-',1+Z,zpi,'-');
ylim([-1 1.5])
set(gca,'XDir','reverse');
```

Bibliography

[1] E. Komatsu *et al.* [WMAP Collaboration], "Five-Year Wilkinson Microwave Anisotropy Probe (WMAP) Observations:Cosmological Interpretation," [arXiv:astro-ph/0803.0547].

[2] M. S. Turner, and D. Huterer, "Cosmic acceleration, dark energy and fundamental physics," [arXiv:astro-ph/0706.2186].

[3] A. G. Riess *et al.* [Supernova Search Team Collaboration], Observational Evidence from Super- novae for an Accelerating Universe and a Cosmological Constant, Astron. J. **116**, 1009 (1998); S. Perlmutter *et al.* [Supernova Cosmology Pro ject Collaboration], Measurements of Omega and Lambda from 42 High-Redshift Supernovae, Astrophys. J. **517**, 565 (1999).

[4] W. J. Percival *et al.*, "Measuring the matter density using baryon acoustic oscillations in the Sloan Digital Sky Survey," MNRAS, **327**, 1297 (2001).

[5] J. P. Ostriker and P. J. Steinhardt, "Cosmic concordance," [arXiv:astro-ph/9505066].

[6] M. Tegmark *et al.* [Sloan Digital Sky Survey], "Cosmological parameters from SDSS and WMAP," Phys. Rev. D **69**, 103501 (2004)

[7] R. Rebolo *et al.* [Very Small Array Collaboration], "Cosmological parameter estimation using Very Small Array data out to l=1500," Monthly Notices of the Royal Astronomical Society, Volume 353, Issue 3, pp. 747-759

[8] G. R. Dvali, G. Gabadadze and M. Porrati, "4D gravity on a brane in 5D Minkowski space," Phys. Lett. B **485**, 208 (2000) [arXiv:hep-th/0005016].

[9] G. W. Gibbons, and S. W. Hawking, "Action integrals and partition functions in quantum gravity," Phys. Lett. D **15**, 2752 (1977); S. W. Hawking, and G. T. Horowitz, "The graviational hamiltonian, action, entropy, and surface terms," Class. Quant. Grav. **13**, 1487 (1996) [arXiv:hep-th/0005016].

[10] G. R. Dvali, A. Gruzinov and M. Zaldarriaga, "The accelerated universe and the Moon," Phys. Rev. D **68**, 024012 (2003) [arXiv;hep-th/0212069].

[11] M. Fierz and W. Pauli, "On relativistic wave equations for particles of arbitrary spin in an electromagnetic field," Proc. Roy. Soc. Lond. A **173**, 211 (1939).

[12] C. Brans and H. Dicke, "Mach's Principle and a Relativistic Theory of Gravitation,', Phys. Rev. **124**, 925 (1961); R. H. Dicke, "Mach's Principle and invariance under transformation of units," Phys. Rev. **125**, 2163 (1962); P. G. Bergmann, "Comments on the scalar tensor theory," Int. J. Theor. Phys. **1**, 25 (1968).

[13] H. van Dam and M. J. G. Veltman, "Massive And Massless Yang-Mills And Gravitational Fields," Nucl. Phys. B **22**, 397 (1970); V. I. Zakharov, "Linearized gravitation theory and the graviton mass," JETP Lett. **12**, 312 (1970);

[14] A. I. Vainshtein, "To the problem of nonvanishing gravitation mass," Phys. Lett. B **39**, 393 (1972).

[15] C. Deffayet, G. R. Dvali, G. Gabadadze and A. I. Vainshtein, "Nonperturbative continuity in graviton mass versus perturbative discontinuity," Phys. Rev. D **65**, 044026 (2002) [arXiv;hep-th/0106001].

[16] A. Gruzinov, "On the graviton mass," New Astron. **10**, 311 (2005) [arXiv:astro-ph/0112246].

[17] M. Porrati, "Fully covariant van Dam-Veltman-Zakharov discontinuity, and absence thereof," Phys. Lett. B **534**, 209 (2002) [arXiv:hep-th/0203014].

[18] C. Deffayet, "Cosmology on a brane in Minkowski bulk," Phys. Lett. **B 502**, 199 (2001) [arXiv:hep-th/0010186].

[19] M. A. Luty, M. Porrati, and R. Rattazzi, "Strong interactions and stability in the DGP model," JHEP **0309**, 029 (2003) [arXiv:hep-th/0303116].

[20] A. Nicolis and M. Rattazzi, "Classical and quantum consistency of the DGP model," JHEP **0309**, 029 (2003) [arXiv:hep-th/0303116].

[21] C. Charmousis, R. Gregory, N. Kaloper and A. Padilla, "DGP specteroscopy," JHEP **0610**, 066 (2006) [arXiv:hep-th/0604086].

[22] G. Dvali, G. Gabadadze, O. Pujolas and R. Rahman, "Domain walls as probes of gravity," Phys. Rev. D **75**, 124013 (2007) [arXiv:hep-th/0612016].

[23] R. Gregory, N. Kaloper, R. C. Myers and A. Padilla, "A New Perspective on DGP Gravity," JHEP **0710**, 069 (2007) [arXiv:hep-th/0707.2666].

[24] K. Izumi, K. Koyama, O. Pujolas and T. Tanaka, "Bubbles in the Self-Accelerating Universe," Phys. Rev. D **76**, 104041 (2007).

[25] A. Lue, R. Scoccimarro and G. D. Starkman, "Probing Newton's constant on vast scales: DGP gravity, cosmic acceleration and large scale structure," Phys. Rev. D **69**, 124015 (2004) [arXiv:astro-ph/0401515].

[26] K. Koyama and R. Maartens, "Structure formation in the DGP cosmological model," JCAP **0601**, 016 (2006) [arXiv:astro-ph/0511634].

[27] I. Sawicki, Y. S. Song and W. Hu, "Near-horizon solution for DGP perturbations," Phys. Rev. D **75**, 064002 (2007) [arXiv:astro-ph/0606285].

[28] M. Ishak, A. Upadhye and D. N. Spergel, "Probing cosmic acceleration beyond the equation of state: Distinguishing between dark energy and modified gravity models," Phys. Rev. D **74**, 043513 (2006) [arXiv:astro-ph/0507184]. M. Fairbairn and A. Goobar, "Supernova limits on brane world cosmology," Phys. Lett. B **642**, 432 (2006) [arXiv:astro-ph/0511029]; R. Maartens and E. Majerotto, "Observational constraints on self-accelerating cosmology," Phys. Rev. D **74**, 023004 (2006) [arXiv:astro-ph/0603353]; S. Wang, L. Hui, M. May and Z. Haiman, "Is Modified Gravity Required by Observations? An Empirical Consistency Test of Dark Energy Models," Phys. Rev. D **76**, 063503 (2007) [arXiv:astro-ph/0705.0165].

[29] Y. S. Song, I. Sawicki and W. Hu, "Large-scale tests of the DGP model," Phys. Rev. D **75**, 064003 (2007) [arXiv:astro-ph/0606286].

[30] W. Fang, S. Wang, W. Hu, Z. Haiman, L. Hui and M. May, "Challenges to the DGP Model from Horizon-Scale Growth and Geometry," [arXiv:astro-ph/0808.2208].

[31] "Cosmological Evidence for Extra Dimensions", N. Afshordi, G. Geshnizjani and J. Khoury, to appear.

[32] N. Arkani-Hamed, H. Georgi and M. D. Schwartz, "Effective field theory for massive gravitons and gravity in theory space," Annals Phys. **305**, 96 (2003).

[33] M. A. Luty, M. Porrati and R. Rattazzi, "Strong interactions and stability in the DGP model," JHEP **0309** (2003) 029.

[34] A. Lue and G. D. Starkman, "How a brane cosmological constant can trick us into thinking that W < -1," Phys. Rev. D **70**, 101501 (2004) [arXiv:astro-ph/0408246]; V. Sahni and Y. Shtanov, "Braneworld models of dark energy," JCAP **0311**, 014 (2003) [arXiv:astro-ph/0202346]; L. P. Chimento, R. Lazkoz, R. Maartens and I. Quiros, "Crossing the phantom divide without phantom matter," JCAP **0609**, 004 (2006) [arXiv:astro-ph/0605450].

[35] G. R. Dvali, "Predictive power of strong coupling in theories with large distance modified gravity," New J. Phys. **8**, 326 (2006) [arXiv:hep-th/0610013].

[36] G. R. Dvali, S. Hofmann, and J. Khoury, "Dgravitation of the cosmological constant and graviton," Phys. Rev. D **76**, 084006 (2007) [arXiv:hep-th/0209227].

[37] A. Nicolis, M. Rattazzi, and E. Trincherini, "The galileon as a local modification of gravity," [arXiv:hep-th/0811.2197].

[38] A. Adams, *et al.* "Causality, analyticity and an IR obstruction to UV completion," [arXiv:hep-th/0602178].

[39] R. M. Wald, "General Relativity" (The University of Chicago Press) 1984.

[40] J. P. Kneller and G. Steigman, "BBN and CMB constraints on dark energy," Phys. Rev. D **67**, 063501 (2003) [arXiv:astro-ph/0210500v2].